CHEMICAL MASS TRANSFER AND SOLUTION FLOW IN WYOMING ROLL-TYPE URANIUM DEPOSITS

by

Regina Marie Capuano

A Thesis Submitted to the Faculty of the

DEPARTMENT OF GEOSCIENCES

In Partial Fulfillment of the Requirements
For the Degree of

MASTER OF SCIENCE

In the Graduate College

THE UNIVERSITY OF ARIZONA

1 9 7 7

STATEMENT BY AUTHOR

This thesis has been submitted in partial fulfillment of requirements for an advanced degree at The University of Arizona and is deposited in the University Library to be made available to borrowers under rules of the Library.

Brief quotations from this thesis are allowable without special permission, provided that accurate acknowledgment of source is made. Requests for permission for extended quotation from or reproduction of this manuscript in whole or in part may be granted by the head of the major department or the Dean of the Graduate College when in his judgment the proposed use of the material is in the interests of scholarship. In all other instances, however, permission must be obtained from the author.

SIGNED: Regina Marie Lyman

APPROVAL BY THESIS DIRECTOR

This thesis has been approved on the date shown below:

Dec 12/77

Denis L. Norton
Associate Professor of Geosciences

Date

ACKNOWLEDGMENTS

I wish to express my deepest gratitude to my advisor, Dr. Denis L. Norton, for his guidance, patience, and understanding through this study. I also thank Jerry Knight, Richard Knapp, Ken Bladh, and Leslie McFadden for encouragement, friendship, and many useful discussions. Dr. John Anthony and Dr. Austin Long I thank for serving on my thesis committee and reviewing this manuscript.

This research was supported by Wyoming Minerals Corp., which I gratefully acknowledge; in particular, I thank Harry Noyes for many useful suggestions. I also wish to express thanks to Dr. C. F. Baes, Chemist, Union Carbide Corp., and Dr. V. B. Parker, Chemist, National Bureau of Standards, for discussion of data, to Utah International for a tour of the Lucky Mc Mine, and to Lynn McLean for improvements in the manuscript.

TABLE OF CONTENTS

LIST OF ILLUSTRATIONS

LIST OF ILLUSTRATIONS--Continued

LIST OF TABLES

ABSTRACT

Two processes of uranium roll formation have been studied using current thermochemical data and computations of irreversible mass transfer between fluids and rocks for the system UO_2-UO_3-CaO-K_2O-MgO-Fe_2O_3-FeO-Al_2O_3-SiO_2-H_2S-SO_4-H_2O-CO_2. One mechanism of formation is the result of an oxidized, acidic, uranium-bearing groundwater (log f_{O_2} = -30.0, pH = 6.0, log f_{CO_2} = -1.5, log ΣM_U = -7.0) infiltrating into a reduced zone in the sandstone through which it flows, reacting with the pyrite, biotite, quartz, feldspar, and calcite. These calculations indicate that this mechanism of ore formation is effective over relatively short distances of solution influx, as a result of rapid reduction of the solution through the dissolution of pyrite and biotite. The other mechanism studied is that of ore formation as a reduced, uranium-bearing carbonate groundwater (log f_{O_2} = -68.1, pH = 9.0, log f_{CO_2} = -2.1, log ΣM_U = -5.4) flowing into and reacting with the kaolinite and hematite in an altered sandstone, or mixing with an acidic groundwater. This mechanism of ore formation suggests the possible localization of uranium ore deposits at the margins of closed saline basins containing high carbonate groundwaters.

INTRODUCTION

Chemical processes which form Wyoming roll-type uranium deposits consist of reactions between circulating groundwaters and the host rocks. In this study, the mechanism of formation of these ore bodies and the composition of possible ore-forming solutions was examined by numerical simulation of solution-mineral reactions using current thermochemical data for uranium minerals and aqueous species.

Uranium roll-type deposits are generally characterized as crescent-shaped bodies occurring in gently-dipping, permeable arkosic sandstone units of Tertiary age. The sandstone host is bounded by less permeable units and is interlayered with silt or claystone lenses. Some deposits occupy the entire sandstone interval between the two impermeable beds; others occupy only a portion of that interval. As seen in plan section, the ore typically occurs as tongue-shaped units extending several kilometers in length and tens of meters in width, while in cross-section they may be several meters high and crescent-shaped, cutting sharply across host rock bedding. The physical and chemical characteristics of these deposits have been described by many authors (Shawe and Granger, 1965; Adler and Sharp, 1967; Harshman, 1968a, 1974; Files, 1970; Fischer, 1970; Adler, 1974; and

Granger and Warren, 1974), as have the physical and chemical characteristics of the deposits of specific regions, such as Gas Hills (King and Austin, 1966; Anderson, 1969; Armstrong, 1970), the Powder River Basin (Mrak, 1968; Davis, 1969; Dahl and Hagmair, 1974), the Shirley Basin (Melin, 1969; Harshman, 1962, 1968b, 1972), Crooks Gap (Bailey, 1969), or the Black Hills (Hart, 1968; and Renfro, 1969).

These authors have generally noted that there are two zones in the sandstone associated with ore deposition: (1) a bleached and often iron oxide-stained sandstone occurring on the concave side of the ore body and (2) an unaltered, unmineralized arkosic sandstone occurring on the convex side (figure 1). The bleached, altered sandstone on the concave side of the ore roll varies widely in size but is typically a few tens of meters thick, a few kilometers wide, and 10 kilometers more or less long (Harshman, 1974). It contains little or no pyrite, calcite cement, or organic matter, and biotite originally present in the sandstone is altered.

The bleached appearance is believed due to greater clay alteration in this zone than in the unaltered sandstone, but, according to Files (1970), the occurrence of the clay minerals, kaolinite, montmorillonite, chlorite, and illite, is the same on both sides of the roll, suggesting

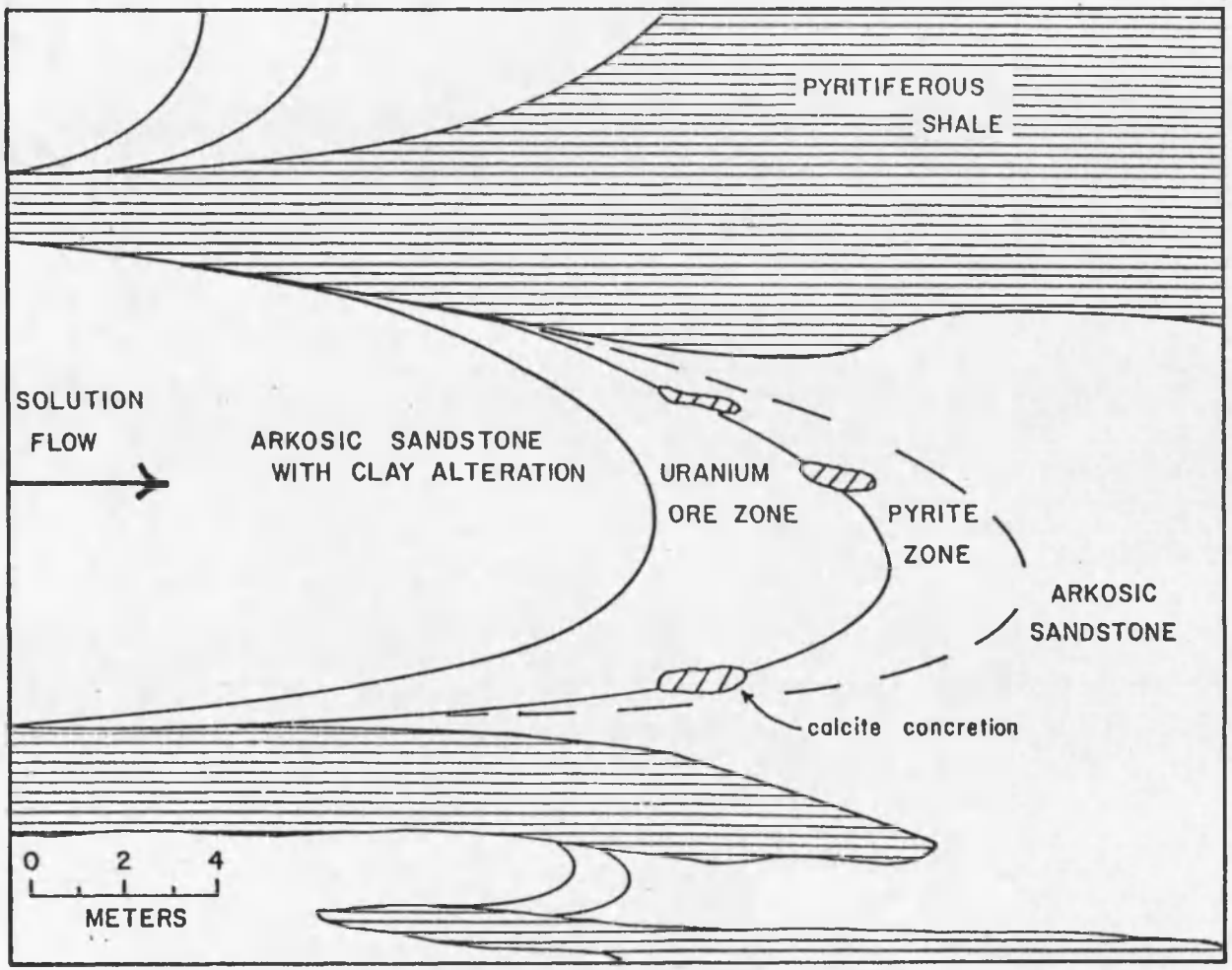

Figure 1. Idealized cross-section through uranium ore roll, based on Granger and Warren (1974) and Harshman (1974).

that this mineral assemblage may not be associated with ore formation. The only exception which Files (1970) noted, but had no explanation for, is the occurrence of whitened rinds surrounding pink cores on orthoclase grains in the bleached sandstone. A zone of very bleached or limonitic stained sandstone, ranging in thickness from less than 1 cm to a few hundred meters, borders the contact between altered sandstone and the ore zone (Granger and Warren, 1974). This zone, in some cases, contains a small concentration of pyrite that is either obviously the altered or euhedral and unaltered variety. At the contact between altered sandstone and the ore zone, which is fairly distinct, a selenium-rich zone extends several centimeters into each region.

The ore zone, which generally occurs below the groundwater table, has concentrations of U_3O_8 ranging from 0.1 to a few weight percent, with the highest concentration occurring closest to the altered sandstone contact. Uraninite and coffinite are the most common uranium minerals in these ore bodies; they are found coating sand grains and filling interstitial spaces. Pyrite and organic material, up to several weight percent, usually fill interstitial spaces in the sandstone, while calcite forms concretionary-like masses. On the convex side of the rolls this uranium ore zone grades into barren unaltered sandstone, with ore

stage pyrite commonly extending beyond uraninite occurrences. Unaltered sandstone is typically light gray to pale brown and contains up to 2 weight percent disseminated syngenetic pyrite, pervasive calcite cement, and organic material.

Formation of the ore zone and associated alteration minerals is attributed to reactions between groundwaters and the host rocks. Based on uranium thermochemical data, the chemical composition of these ore-forming solutions is suggested by Hostetler and Garrels (1962) to have pHs ranging from 6 to 10, Eh ranging from 0.0 to -0.3 volts, and a total carbonate concentration of 10^{-2} molal, at temperatures less than $100^{\circ}C$ and 1 atmosphere pressure. Uranium found in these mineralizing solutions is believed to be derived through leaching of either uranium-bearing Pre-Cambrian granite (Stuckless et al., 1977), arkosic host beds (Melin, 1964; King and Austin, 1966; and Rosholt and Bartel, 1969), or uranium-bearing tuffaceous material in overlying beds (Love, 1952; and Denson, Bachman, and Zeller, 1959). It is generally accepted that as this uranium-bearing solution flowed into a more reducing environment, uranium minerals deposited, forming a crescent-shaped ore zone which is concave toward the assumed direction of flow. Continued resolution and deposition of uranium by subsequent solutions causes the roll to migrate in the direction of solution flow

and to increase in grade (Gruner, 1956; Rosholt et al., 1964; Warren, 1971; and Warren and Granger, 1973).

Several mechanisms for precipitation of uranium from the ore-forming solution have been suggested. One method employs biologic activity and is based on the investigation of sulfur isotopes of pyrite associated with the ore body. Such studies have indicated a sharp change in δS^{34} values across the roll front (Jensen, 1958; Cheney and Jensen, 1966; and Austin, 1970). According to this model, the isotopic fractionation occurred as a result of the reduction of sulfate by bacteria, which suggests that the roll front was a zone of bacterial activity. Granger and Warren (1969), however, showed that reconstitution of the diagenetic pyrite should result in isotopic fractionation of the sulfur and that the process of roll formation could probably lead to the δS^{34} values observed, without any bacterial action. Studies by Warren (1971, 1972) and Cheney and Trammell (1973) support this chemical, non-biogenic, origin, which requires reactions between the solution and host rock to produce a zone having a steep Eh gradient. Files (1970) suggested a combined biological and geochemical origin in which pyrite and bacterial action reduce the solution, while Granger and Warren (1974) propose a geochemical origin in which a ferric thiosulphate complex is formed ($Fe(S_2O_3)^+$), which, when

reacted with pyrite, is thought to produce the steep Eh gradient at the roll front. Spirakis (1977) has recently suggested that the chemical interface is a product of a semi-permeable membrane formed through the deposition of clay minerals in the ore zone. Differential diffusion of ions across this membrane could produce an acid sulfate and a basic carbonate solution on opposite sides of the membrane. He proposes that a pH difference across this interface allows ore formation in the region of the sulfate solution while the environment of the carbonate solution is barren.

Chemical processes that form Wyoming roll-type uranium deposits apparently consist of equilibrium and non-equilibrium reactions between circulating groundwaters and the host rock. A numerical simulation of these mass transfer reactions, in conjunction with updated thermodynamic data for uranium minerals and aqueous species, makes it possible to predict the composition of these ore-forming solutions and the mechanisms of roll formation, including the mineral zoning sequence produced and the abundances of ore and gangue minerals precipitated. Through calculation of the molalities and activities of all species in a given solution of varying composition, using a numerical simulation of mass balance and mass action equations that define equilibrium conditions in an aqueous solution (Knight, 1976),

it was possible to determine the affect of aqueous complexes on uranium solubility.

Based on a series of solution equilibrium calculations, combined with geologic observations compiled from the literature, the ore-forming solution is suggested in this study to have a composition similar to an acid arkosic groundwater or a carbonate groundwater near equilibrium with a pyrite-bearing sandstone. Reactions between these solution compositions and the country rock, that would cause deposition of uranium ore bodies and the alteration gangue minerals, were simulated by calculation of the mass transfer between these groundwaters and host rock. Numerical methods used in this study are similar to those employed by Helgeson (1970) in his study of the formation of alteration zones associated with hydrothermal systems. The results of the numerical simulation of reactions between both acid groundwaters and bicarbonate groundwaters with the country rock indicate that the zoning associated with these deposits can, indeed, be produced by reactions with either solution.

Data required for the analysis of uranium ore roll forming processes includes (1) a general description of these ore bodies, (2) a current data base containing the available thermochemical data for uranium species and minerals, (3) kinetic data for calcite, feldspar, and biotite,

in order to determine their relative reaction rates, and (4) kinetic data for uraninite in order to calculate its rate of dissolution into circulating groundwaters.

URANIUM THERMOCHEMICAL DATA

Thermodynamic data of uranium minerals and aqueous species, relevant to predicting uranium solubility in the natural environments, are compiled in tables 1, 2, and 3. Equilibrium constants were calculated for the hydrolysis and dissociation reactions of uranium minerals and aqueous species at 25°C, 1 atmosphere, and 1 molal standard state, on the basis of data taken from the literature. Uranium equilibrium constants are consistent with Helgeson's (1969) data compilation, from which equilibrium constants for minerals and aqueous species other than uranium were taken directly.

Oxides and Hydroxides

The dominant uranium valence states in natural waters are (IV) and (VI). They occur in solution as U^{+4} and UO_2^{++}. Fuger and Oetting (1976) have recently determined the thermodynamic constants for these species. Their data, which are considerably different from previously accepted values (Rossini et al., 1952; Latimer, 1952; Garrels and Christ, 1965; and Wagman et al., 1971), were used in this study.

Hydrolysis of U^{+4} has been reviewed by Baes and Mesmer (1976), who also calculated the dissociation constants

Table 1. Thermodynamic Constants for Uranium Solids and Aqueous Species

SUBSTANCES	State	S^o cal/deg mole	ΔH^o_f kcal/mole	ΔG^o_f kcal/mole	Reference
OXIDES, HYDROXIDES					
U^{+3}	aq	-41.8±2.0	-116.9±0.9	-114.9±1.1	Fuger and Oetting, 1976
UO_2^+	aq	-6.±2.	-246.8±1.4	-231.5±1.3	Fuger and Oetting, 1976
U^{+4}	aq	-99.±5.	-141.3±0.8	-126.9±0.5	Fuger and Oetting, 1976
UOH^{+3}	aq	-46.	-197.92	-182.7	Baes and Mesmer, 1976
$U(OH)_2^{++}$	aq			(-237.7)	Baes and Mesmer, 1976[1]
$U(OH)_3^+$	aq			(-291.3)	Baes and Mesmer, 1976[1]
$U(OH)_4^o$	aq			(-343.1)	Baes and Mesmer, 1976[1]
$U(OH)_5^-$	aq			-392.6	Baes and Mesmer, 1976[1]
UO_2^{++}	aq	-23.2±0.9	-243.5±0.4	-227.7±0.5	Fuger and Oetting, 1976
UO_2OH^+	aq	4.51	-300.82	-276.5	Baes and Mesmer, 1976
$(UO_2)_2(OH)_2^{++}$	aq			-561.1	Baes and Mesmer, 1976
$(UO_2)_3(OH)_5^+$	aq			-945.2	Baes and Mesmer, 1976
U	C	12.03 12.00±.03	0 0	0 0	Jones, Gordon, and Long, 1952 Flotow and Lohr, 1960; Oetting, Rand, and Ackerman, 1976
UO_2 [Uraninite]	C	18.63 18.41 18.41±.05	 -259.3 -259.32±.02	-246.6±0.6 -246.7	Jones, Gordon, and Long, 1952 Huntzicker and Westrum, 1971 Huber and Holley, 1969 Parker, V. B., 1977, private communication Fuger and Oetting, 1976
UO_2	Amp			(-233.7)	Langmuir and Applin, 1977
$UO_{2.67}$	C	22.51	-284.8	-268.5	Parker, V. B., 1977, private communication

Table 1. Thermodynamic Constants (cont'd.)

SUBSTANCES	State	S^o cal/deg mole	ΔH^o_f kcal/mole	ΔG^o_f kcal/mole	Reference
U_3O_8	C		-854.5		Huber and Holley, 1969
		67.53			Westrum and Grønvold, 1959
				-804.	Deltombe, de Zoubov, and Pourbaix, 1956
		66.	-853.5	-804.	Seaborg and Katz, 1954
UO_3	C		β -291.6		Cordfunke, Ouweltjes, and Prins, 1975
			γ -292.5		Cordfunke, Ouweltjes, and Prins, 1975
		23.57		-273.1	Jones, Gordon, and Long, 1952
		23.6	-291.6	-273.1	Seaborg and Katz, 1954
		22.97		-273.9	Parker, V. B., 1977, private communication
UO_3	Amp		-288.5		Fuger and Oetting, 1976
$UO_2(OH)_2$	C		-366.15		Drobnič and Kolar, 1966[1]
			-368.7		Cordfunke, 1964
				-332.8±1.1	Nikitin et al., 1972[1]
				-333.4	Baes and Mesmer, 1976 + Gayer and Leider, 1955
		-42.			Baes and Mesmer, 1976 + Gayer and Leider, 1955 + Cordfunke, 1964
		-51.			Baes and Mesmer, 1976 + Gayer and Leider, 1955 + Drobnič and Kolar, 1966[2]
$UO_2(OH)_2 \cdot H_2O$ [Schoepite]	C		-436.0±2.		Drobnič and Kolar, 1966
			-438.6		Cordfunke, 1964
				-389.6±1.1	Nikitin et al., 1972[1]
		32.6			Nikitin et al., 1972 + Cordfunke, 1964
CARBONATES					
$UO_2CO_3^o$	aq	5.	-406.4	-367.4	Sergeyeva et al., 1972
$UO_2(CO_3)_2^=$	aq			-502.9	Sergeyeva et al., 1972
$UO_2(CO_3)_3^{-4}$	aq			-636.4	O'Cinnéide, Scanlan, and Hynes, 1972[2]; Tsymbal, 1969[2]
UO_2CO_3	C			-373.4	Sergeyeva et al., 1972
[Rutherfordine]		29.	-405.2		Sergeyeva et al., 1972 + Drobnič and Kolar, 1966[1]
		21.	-407.7		Sergeyeva et al., 1972 + Cordfunke, 1964
SULFATES					
$UO_2SO_4^o$	aq	13.	-455.7	-409.3	Wallace, 1967

Table 1. Thermodynamic Constants (cont'd.)

SUBSTANCES	state	S^o cal/deg mole	ΔH^o_f kcal/mole	ΔG^o_f kcal/mole	Reference
$UO_2(SO_4)_2^=$	aq	29.	-671.1	-588.1	Wallace, 1967
$U(SO_4)_2 \cdot 4H_2O$	c		-836.±2.0		Vidavskii and Ippolitova, 1972
$U(SO_4)_2 \cdot 8H_2O$	c		-1117.8±2.0		Vidavskii and Ippolitova, 1972
CHLORIDES					
UCl^{+3}	aq	-46.	-168.3	-157.1	Naumov, Ryzhenko, and Khodakovsky, 1974
UCl_2^{+2}	aq			-190.6	Goldenberg and Amis, 1959 + Naumov, Ryzhenko, and Khodakovsky, 1974
UO_2Cl^+	aq	-4.5	-282.2	-259.4	Naumov, Ryzhenko, and Khodakovsky, 1974
UCl_3	c	(37.99)	(-213.0)	(-196.9)	Latimer, 1952
UCl_4	c	(47.4)	(-251.2) -243.3 -243.3	(-230.0)	Latimer, 1952 Fitzgibbon, Pavone, and Holley, 1972 Cordfunke, Ouweltjes, and Prins, 1976
UCl_5	c	(62.)	(-261.1)	(-237.4)	Latimer, 1952
UCl_6	c	(68.3)	(-272.4)	(-241.5)	Latimer, 1952
UO_2Cl_2	c	35.98±.05	-300 -291.4 -297.2	-277	Greenberg and Westrum, 1956 O'Hare et al., 1972 Cordfunke, Ouweltjes, and Prins, 1976
SILICATES					
$USiO_4$ [Coffinite]	c	(28.4)	(-478.)	(-456.6) (-452.)	Brookins, 1976 Langmuir and Applin, 1977
$USiO_4$	am			(-439.2)	Langmuir and Applin, 1977

[1]The value taken from the reference cited has been recalculated in this study.

[2]The value taken from the reference cited has been calculated to zero ionic strength in this study.

Table 2. Dissociation Constants for Uranium Aqueous Species

DISSOCIATION REACTIONS	log K 25°C	ΔS_R (25°C) cal/deg mole	ΔH_R (25°C) kcal/mole	ΔG_R (25°C) kcal/mole	Reference
HYDROXIDE					
$UOH^{+3} + H^+ \rightleftarrows U^{+4} + H_2O$	.68±.04 .65±.04	-36. -36.	-11.7 -11.7	-.9 -.9	Kraus and Nelson, 1955 Baes and Mesmer, 1976
	(-10.7±1)	-33.		-.92	Betts, 1955
$U(OH)_2^{+2} + 2H^+ \rightleftarrows U^{+4} + 2H_2O$	(1.9)			-2.6	Baes and Mesmer, 1976[1]
$U(OH)_3^+ + 3H^+ \rightleftarrows U^{+4} + 3H_2O$	(4.2)			-5.7	Baes and Mesmer, 1976[1]
$U(OH)_4^o + 4H^+ \rightleftarrows U^{+4} + 4H_2O$	(7.8)			-10.6	Baes and Mesmer, 1976[1]
$U(OH)_5^- + 5H^+ \rightleftarrows U^{+4} + 5H_2O$	13.0			-17.7	Baes and Mesmer, 1976[1]
$UO_2OH^+ + H^+ \rightleftarrows UO_2^{++} + H_2O$	5.8	-11.	-11.	-7.91	Baes and Mesmer, 1976
$(UO_2)_2(OH)_2^{++} + 2H^+ \rightleftarrows 2UO_2^{++} + 2H_2O$	5.62			-7.67	Baes and Mesmer, 1976
$(UO_2)_3(OH)_5^+ + 5H^+ \rightleftarrows 3UO_2^{++} + 5H_2O$	15.63 15.4 15.42			-21.32	Baes and Mesmer, 1976 Cole et al., 1967[2] Tsymbal, 1969[2]
CARBONATE					
$UO_2CO_3^o \rightleftarrows UO_2^{++} + CO_3^=$	-9.9±.2	48.8	1.1	13.5	Sergeyeva et al., 1972
$UO_2(CO_3)_2^= \rightleftarrows UO_2^{++} + 2CO_3^=$	-16.8±.2 -17.0±.2 -18.2			22.9	Sergeyeva et al., 1972 Tsymbal, 1969[2] McClaine, Bullwinkel, and Huggins, 1955 + Sergeyeva et al., 1972
$UO_2(CO_3)_3^{-4} \rightleftarrows UO_2^{++} + 3CO_3^=$	-21.4 -23.9 -22.1 -22.1 -22.5			30.1 30.1	Sergeyeva et al., 1972 Klygin and Smirnova, 1959[2] O'Cinnéide, Scanlan, and Hynes, 1972[2] Tsymbal, 1969[2] McClaine, Bullwinkel, and Huggins, 1955 + Sergeyeva et al., 1972

Table 2. Dissociation Constants (cont'd.)

DISSOCIATION REACTIONS	log K 25°C	ΔS_R (25°C) cal/deg mole	ΔH_R (25°C) kcal/mole	ΔG_R (25°C) kcal/mole	Reference
SULFATE					
$UO_2SO_4^0 \rightleftarrows UO_2^{++} + SO_4^{=}$	-3.14±.03		-5.1±0.4		Wallace, 1967
	-3.16				Wallace, 1967 + Ahrland, 1951
	-2.3				Allen, 1958[2]
	-1.8			3.71	Kraus and Nelson, 1959[2]
$UO_2(SO_4)_2^{=} \rightleftarrows UO_2^{++} + 2SO_4^{=}$	-4.21±.09		-7.0±0.9		Wallace, 1967
	-4.10				Wallace, 1967 + Ahrland, 1951
	-2.8				Allen, 1958[2]
	-3.11			5.73	Kraus and Nelson, 1959[2]
CHLORIDE					
$UCl^{+3} \rightleftarrows U^{+4} + Cl^-$	-.85			1.16	Kraus and Nelson, 1950
	-.8			1.09	Sobkowski, 1961
	.86	-39.5	-13.0	-1.17	Naumov, Ryzhenko, and Khodakovsky, 1974
$UCl_2^{+2} \rightleftarrows U^{+4} + 2Cl^-$	-.7			1.0	Goldenberg and Amis, 1959 + Naumov, Ryzhenko, and Khodakovsky, 1974
$UO_2Cl^+ \rightleftarrows UO_2^{++} + Cl^-$	-.38			.52	Nelson and Kraus, 1951
	-.22			.30	Bale et al., 1957
	-.21			.29	Davies and Monk, 1957
	-.24	-5.2	-1.25	.328	Naumov, Ryzhenko, and Khodakovsky, 1974

[1]The value taken from the reference cited has been recalculated in this study.

[2]The value taken from the reference cited has been calculated to zero ionic strength in this study.

Table 3. Hydrolysis Constants for Uranium Solid Phases

HYDROLYSIS REACTIONS	log K 25°C	ΔS_R (25°C) cal/deg mole	ΔH_R (25°C) kcal/mole	ΔG_R (25°C) kcal/mole	Reference
HYDROXIDE					
$UO_{2(c)} + 4H^+ \rightleftarrows U^{+4} + 2H_2O$	-4.7 -4.7	-84.0	-18.61	6.4 6.4	Fuger and Oetting, 1976 Parker, V. B., 1977, private communication
$UO_2(OH)_{2(c)} + 2H^+ \rightleftarrows UO_2^{++} + 2H_2O$	5.6±1.5			-7.64	Baes and Mesmer, 1976 + Gayer and Leider, 1955
	6.1			-8.3	Nikitin et al., 1972[1]
			β -11.40 -14.0		Cordfunke, 1964 Drobnič and Kolar , 1966
		52.			Baes and Mesmer, 1976 + Gayer and Leider, 1955 + Cordfunke, 1964
		61.			Baes and Mesmer, 1976 + Gayer and Leider, 1955 + Drobnič and Kolar, 1966[1]
$UO_2(OH)_2 \cdot H_2O_{(c)} + 2H^+ \rightleftarrows UO_2^{++} + 3H_2O$	6.0±0.3			-8.2	Nikitin et al., 1972[1]
			-9.83		Cordfunke, 1964
		-5.7			Nikitin et al., 1972 + Cordfunke, 1964
CARBONATE					
$UO_2CO_{3(c)} \rightleftarrows UO_2^{++} + CO_3^=$	-14.3±.2 (-16.)			19.6	Sergeyeva et al., 1972 McClaine, Bullwinkel, and Huggins, 1955 + Nikitin et al., 1972
	-14.3	-58.	2.36	19.6	Sergeyeva et al., 1972 + Cordfunke, 1964
	-14.3	-66.	-.14	19.6	Sergeyeva et al., 1972 + Drobnič and Kolar, 1966[1]
CHLORIDE					
$UCl_{4(c)} \rightarrow U^{+4} + 4Cl^-$			-57.1±.5		Fuger and Oetting, 1976
$UO_2Cl_{2(c)} \rightleftarrows UO_2^{++} + 2Cl^-$	10.	-32.2	-23.	-13.	Greenberg and Westrum, 1956
SILICATE					
$USiO_{4(c)} + 4H^+ \rightleftarrows U^{+4} + H_4SiO_4$	-7.6 -11.0	-84.	-14.3	10.4 15.0	Langmuir and Applin, 1977 Brookins, 1976

[1]The value taken from the reference cited has been recalculated in this study.

for several of the uranium hydroxides. They have the form $U(OH)_x^{4-x}$, with x ranging from 1 to 5. Baes and Mesmer (1976) give the dissociation constant for UOH^{+3} as 0.65±.04 (reaction 1),

$$UOH^{+3} + H^+ \rightleftarrows U^{+4} + H_2O, \qquad (1)$$

a value derived from reinterpretation of Kraus and Nelson's (1955) data. Baes and Mesmer (1976) also determined a dissociation constant for the species $U(OH)_5^-$ by reinterpreting Gayer and Leider's (1957) experiments, giving a log K = -3.77 for reaction 2,

$$UO_{2\,(c)} + 2H_2O + OH^- \rightleftarrows U(OH)_5^-, \qquad (2)$$

and combining this with reaction 3,

$$UO_{2\,(c)} + 4H^+ \rightleftarrows U^{+4} + 2H_2O \qquad (3)$$

for which a log K = -1.8 was calculated using preliminary thermodynamic data for U^{+4} and $UO_{2\,(c)}$ (N.B.S., private communication, p. 176, in Baes and Mesmer, 1976). From this combination of reactions, a dissociation constant of log K = 16.0 for $U(OH)_5^-$ was obtained (reaction 4).

$$U(OH)_5^- + 5H^+ \rightarrow U^{+4} + 5H_2O. \qquad (4)$$

Baes and Mesmer (1976) then estimated the dissociation constants for the intermediate U^{+4} hydroxides, $U(OH)_2^{++}$, $U(OH)_3^+$,

and $U(OH)_4^o$, assuming a regular progression for the equilibria from UOH^{+3} to $U(OH)_5^-$.

Recent updating of the thermodynamic constants for U^{+4} (Fuger and Oetting, 1976) gives an equilibrium constant for reaction 3 of log K = -4.70 rather than -1.8, as calculated by Baes and Mesmer (1976). A recalculation of Baes and Mesmer's (1976) dissociation constants for the U^{+4} hydroxides, using the current information for U^{+4}, gives the constants listed in table 4.

Baes and Mesmer (1976) also reviewed the hydrolysis of UO_2^{++}, concluding that $(UO_2)_2(OH)_2^{++}$ and $(UO_2)_3(OH)_5^+$ are the dominant hydroxide species at 25°C. The species UO_2OH^+ (Gayer and Leider, 1955) and $(UO_2)_3(OH)_4^{++}$ (Rush, Johnson, and Kraus, 1962) are also suggested as important, but Rush, Johnson, and Kraus (1962) have concluded that UO_2OH^+ is important only at high temperature and that $(UO_2)_3(OH)_4^{++}$ (which they determined must have chloride ions in its structure) is important only in a chloride medium, although they did not state the concentration of chloride necessary. The species $(UO_2)_2(OH)_2^{++}$ and $(UO_2)_3(OH)_5^+$ and their dissociation constants, as determined by Baes and Mesmer (1976), are used in this study.

Uranium oxide phases range in composition from $UO_{2(c)}$ to $UO_{3(c)}$. Thermochemical data for uraninite ($UO_{2(c)}$) were

Table 4. Dissociation Constants for the Uranium (IV) Hydroxides

Reaction	Log K Baes & Mesmer (1976)	Log K Recalculated in this study
$UO_{2(c)} + 4H^+ \rightleftarrows U^{+4} + 2H_2O$	-1.8	-4.7
$UOH^{+3} + H^+ \rightleftarrows U^{+4} + H_2O$	.65	.65
$U(OH)_2^{++} + 2H^+ \rightleftarrows U^{+4} + 2H_2O$	2.6	1.9
$U(OH)_3^{+} + 3H^+ \rightleftarrows U^{+4} + 3H_2O$	5.8	4.2
$U(OH)_4^{o} + 4H^+ \rightleftarrows U^{+4} + 4H_2O$	10.3	7.8
$U(OH)_5^{-} + 5H^+ \rightleftarrows U^{+4} + 5H_2O$	16.0	13.02

determined by Fuger and Oetting (1976) and V. B. Parker (private communication, 1977); these data do not differ greatly from previous calculations (Jones, Gordon, and Long, 1952; Huber and Holley, 1969; and Huntzicker and Westrum, 1971). Since other uranium oxides vary in compositions which range from UO_2 to UO_3 and are not as well characterized, the free energies of formation given by V. B. Parker (communication with Langmuir and Applin, 1977, p. 58), for the phases $UO_{2.67}$ and UO_3, are accepted as the best values.

The important uranium hydroxide phases in natural environments at 25°C are $UO_2(OH)_{2(c)}$ and $UO_2(OH)_2 \cdot H_2O_{(c)}$ (Nikitin et al., 1972; and Baes and Mesmer, 1976). Nikitin et al. (1972) determined the equilibrium constants for $UO_2(OH)_{2(c)}$ and $UO_2(OH)_2 \cdot H_2O_{(c)}$, which were recalculated in this study using the updated thermodynamic constants for UO_2^{++}. Through a reinterpretation of the data of Gayer and Leider (1955), Baes and Mesmer (1976) also calculated an equilibrium constant for $UO_2(OH)_{2(c)}$. Their constant, which does not differ considerably from that of Nikitin et al. (1972), is used in this study, while the constant for $UO_2(OH)_2 \cdot H_2O_{(c)}$ from Nikitin et al. (1972) is used.

Carbonate

Carbonate complexes are thought to be the most important uranium complexes in natural waters (Hostetler and Garrels, 1962). Sergeyeva et al. (1972) performed solubility experiments on $UO_2CO_{3(c)}$ (rutherfordine) and calculated dissociation constants for $UO_2CO_3^o$ and $UO_2(CO_3)_2^{=}$. After reviewing the constants available in the literature, they also predicted a dissociation constant for $UO_2(CO_3)_3^{-4}$. Tsymbal's (1969) dissociation constant for $UO_2(CO_3)_2^{=}$, when recalculated to the same standard state, is in agreement with that of Sergeyeva et al. (1972). Tsymbal (1969) and O'Cinnéide, Scanlan, and Hynes (1972) both calculated a dissociation constant for $UO_2(CO_3)_3^{-4}$, as well. Both of their constants, when recalculated to standard state, were in agreement, although they differ from the values suggested by Sergeyeva et al. (1972). The dissociation constant for $UO_2(CO_3)_3^{-4}$ suggested by Sergeyeva et al. (1972) was Tsymbal's (1969) value which they recalculated to standard state. Sergeyeva et al.'s (1972) equilibrium constant for $UO_2CO_{3(c)}$ and dissociation constants for $UO_2CO_3^o$ and $UO_2(CO_3)_2^{=}$ are used in this study, while the work of Tsymbal (1969) and O'Cinnéide, Scanlan, and Hynes (1972) is used for the dissociation constant of $UO_2(CO_3)_3^{-4}$.

Sulfate, Chloride, and Silicate

The dominant uranium sulfate species are $UO_2SO_4^o$ and $UO_2(SO_4)_2^=$. Dissociation constants for these species (Ahrland, 1951; Allen, 1958; Kraus and Nelson, 1959; and Wallace, 1967) range from -3.2 to -1.8 for $UO_2SO_4^o$ and from -4.2 to -2.7 for $UO_2(SO_4)_2^=$. Wallace (1967) recalculated Ahrland's (1951) dissociation constants to 25°C and standard state and found good agreement between their calculated values. Kraus and Nelson's (1959) constants differ from those of Wallace (1967) and Ahrland (1951), but their paper did not include an explanation of their method. Allen's (1958) constants also differ from those of Wallace (1967) and Ahrland (1951). Wallace's (1967) calculations are believed by the present writer to be the most reliable, and his dissociation constants are used in this study. Lietzke and Stoughton (1960) calculated entropies and enthalpies for these uranium sulfate species, but because they used the dissociation constants given by Kraus and Nelson (1959), their work is not included in this study.

The important uranium chloride species include UO_2Cl^+, which carries uranium in the oxidized state, and the reduced species UCl^{+3} and UCl_2^{++}. A dissociation constant for UO_2Cl^+ was determined experimentally by Nelson and Kraus (1951), Bale et al. (1957), Davies and Monk (1957), and

Naumov, Rhyzhenko, and Khodakovsky (1974). They recorded values ranging from -.38 to -.21. An average of these constants, of log K = -.26, is used. For the species UCl^{+3} the dissociation constant of Naumov et al. (1974) is used, and for UCl_2^{++} the constant of Goldenberg and Amis (1959), combined with Naumov et al.'s (1974) constant, is adopted.

For the uranium silicate phase, coffinite $(U(SiO_4)_{1-x}(OH)_{4x}$, thermodynamic data is available only for the dehydrated form, with x = 0. The ΔG_f for $USiO_4$ given by Brookins (1976) is an approximation using the differences in ΔG_f values of the oxide-silicate pairs of zirconium, thorium, and, thereby, uranium compounds. Langmuir and Applin (1977) did not state their method of calculation of the ΔG_f of $USiO_4$. Langmuir and Applin's (1977) value is used in this study rather than Brookins' (1976) because of the uncertainty of his method.

KINETIC DATA

Irreversible dissolution rates of minerals are calculated, in this study, using the reaction rate law (Aagaard and Helgeson, 1977; and D. L. Norton, unpublished date, 1977):

$$\frac{dc_\alpha}{dt} = k_\alpha S_\alpha a_i^\omega \quad (g/cm^3 \text{ sec})$$

where:

k_α = rate constant for phase α (g/cm^2 sec)

S_α = surface area for phase α per unit volume of fluid (cm^2 per cm^3 of fluid)

c_α = concentration of α^{th} phase per unit volume of fluid (g per cm^3 of fluid)

a_i = activity of i^{th} ion

ω = exponent reflecting order of reaction with respect to i^{th} ion

Reaction rate constants at 25°C and the order of reaction dependency on ion concentrations are listed in table 5.

A reaction rate constant for uraninite is taken from the results of Grandstaff's (1976, p. 1506, samples L25 through L37) experiments on uraninite dissolution in solutions of varying carbonate concentration. The rates $(\frac{dc_\alpha}{dt}/S_\alpha)$

Table 5. Kinetic Constants

Mineral	i	ω	log K_{25^oC} $g/cm^2 sec$
Biotite[1]	H^+	1.2	-9.6
Quartz[1]	-	-	-20.4
Feldspar[2]	H^+	1	-10.8
Calcite[3]	Ca^{++}	.5	-5.1
	$CO_3^=$	.5	
Uraninite[4]	H^+	1	.43
	ΣCO_3	1	

[1]R. Kolvoord and K. Yorgason, 1972, Geochemists, ARCO, unpublished data.

[2]Aagaard and Helgeson, 1977.

[3]Sjöberg, 1976.

[4]Grandstaff, 1976.

he recorded contained the effect of hydrogen ion activity and total carbonate activity, allowing the rate constant to be calculated using the relation

$$k_{uran} = \frac{\frac{dc_{uran}}{dt}}{a_{H^+}\, a_{\Sigma CO_3}} .$$

URANIUM SOLUTION CHEMISTRY

The effects of complexing on uranium solubility in aqueous solutions of varying chemical composition are calculated using the mass balance and mass action equations that define equilibrium conditions in aqueous solutions (Helgeson, Brown, Nigrini, and Jones, 1970; Van Zeggeren and Storey, 1970; and Knight, 1976). Given the pH, temperature, and total molalities of components in a solution, the molalities and activities of all species present in the solution are calculated.

The effect of complexing on the solubility of uranium at 25°C and 1 atmosphere is investigated for an acidic groundwater and for a high carbonate groundwater. Calculations indicate that the carbonate groundwater, with 10^{-1} molal carbonate, would carry two orders of magnitude more uranium in solution than the lower carbonate, acidic groundwater, with 10^{-3} molal carbonate, due to the greater complexing of the uranium carbonate species in the high carbonate solution (figures 2 and 3). It is also noted that a decrease in either pH or oxygen fugacity would produce a reduction in uranium solubility in both solutions, from log $f_{O_2} \approx -45$ to -60 in the acid groundwater, and from log $f_{O_2} \approx -45$ to -70 in the carbonate groundwater.

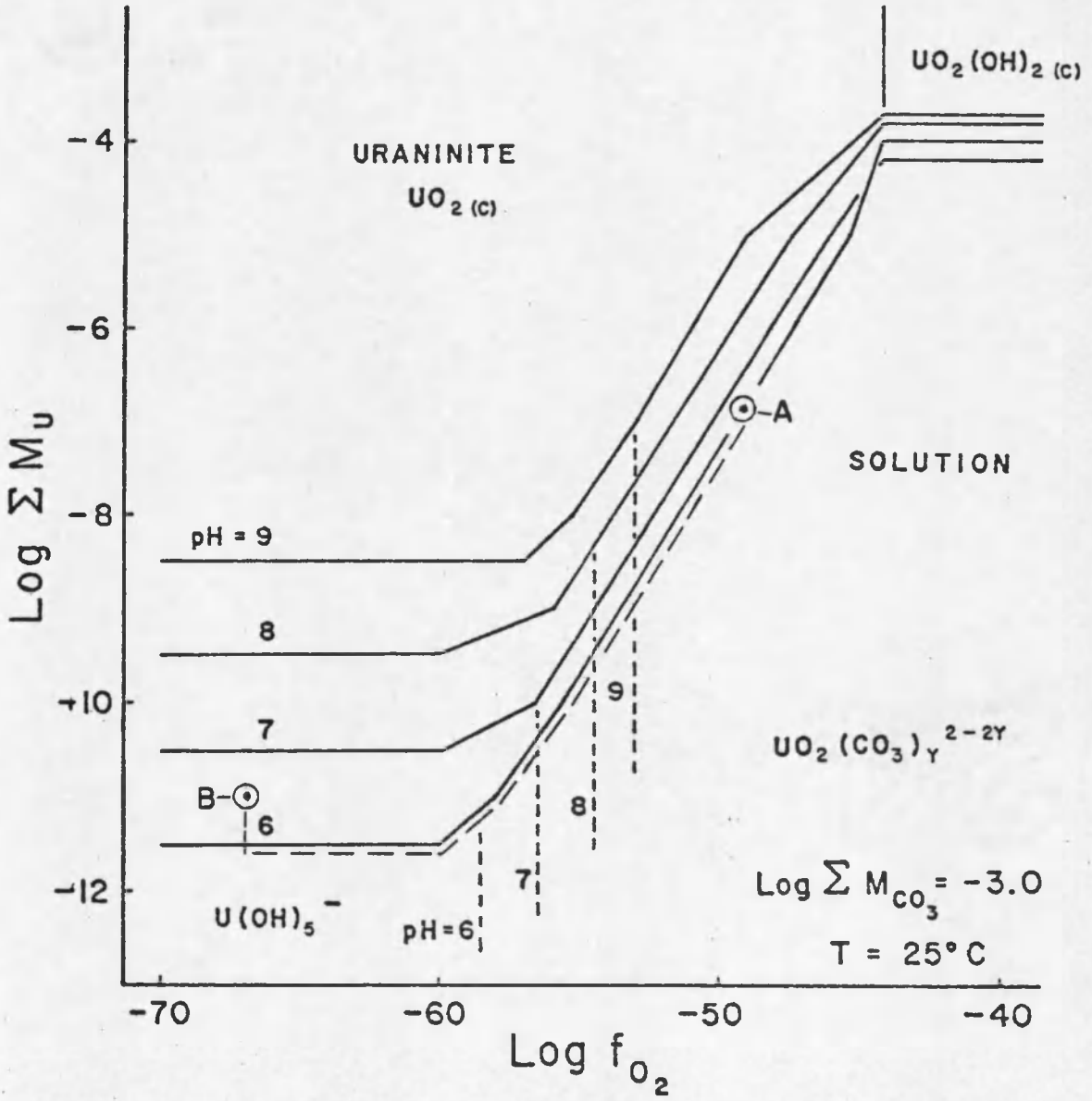

Figure 2. Solution mineral equilibria diagram for solution with log ΣM_{CO_3} = -3.0, T = 25°C, P = 1 bar, a_{H_2O} = 1, a_{solids} = 1, and I = 0.1 molal.

Solid lines are saturation surfaces between minerals and aqueous solutions at varying pHs. Dashed lines indicate that the activities of the dominant aqueous species are equal. Only the dominant species in the solution are listed.

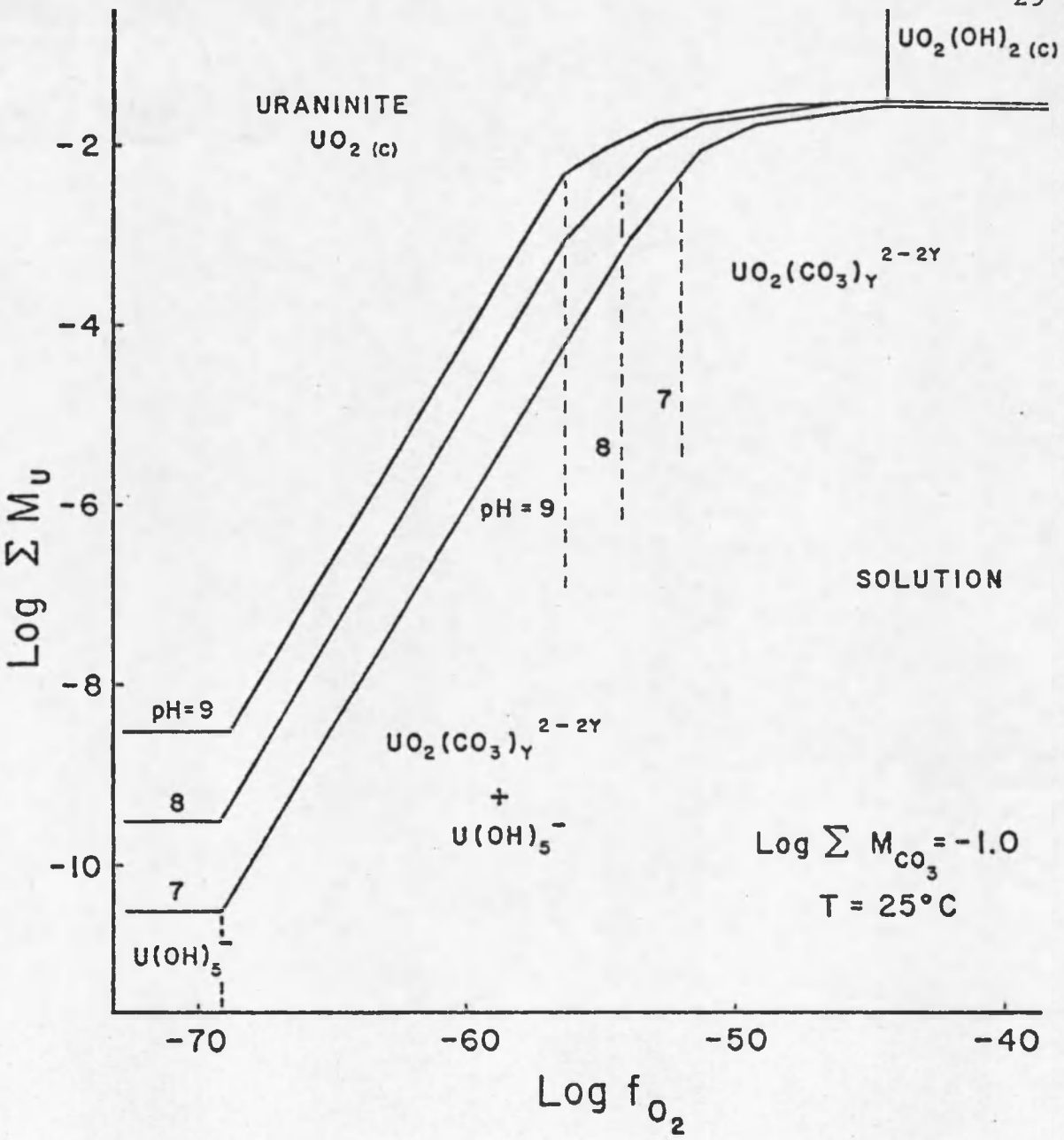

Figure 3. Solution mineral equilibria diagram for a solution containing log ΣM_{CO_3} = -1.0, T = 25°C, P = 1 bar, a_{H_2O} = 1, a_{solids} = 1, and I = 0.1 molal.

Solid lines are saturation surfaces between minerals and aqueous solutions at varying pHs. Dashed lines indicate that the activities of the dominant aqueous species are equal. Only the dominant species in the solution are listed.

Acidic Groundwater

Acid groundwaters in arkosic sandstones contain approximately 10^{-3} molal carbonate and pH values ranging from 6 to 8 (White, Hem, and Waring, 1963; and Paces, 1972). Uranium complexing and solution-mineral equilibria are calculated, for a range in oxygen fugacities and pH, for these groundwaters. In these solutions, uranium complexes with hydroxide and carbonate ions are important, while those with sulfate and chloride ions do not affect uranium solubility significantly, even at relatively high concentrations of total sulfur and chloride.

In reduced groundwaters (log $f_{O_2} \lesssim 10^{-55}$) uranium (IV) hydroxide species control uranium solubility (figure 4). $U(OH)_5^-$ is the dominant complex in these solutions, for the pH range studied (figure 5). Under oxidized conditions the uranium (VI) carbonate species dominate, as shown in figure 4. The most important uranium (VI) carbonate complex from pH $\sim$ 5 to 7 is $UO_2CO_3^o$, from pH $\sim$ 7 to 8 is $UO_2(CO_3)_2^=$, and from pH > 8 is $UO_2(CO_3)_3^{-4}$ (figure 6).

Variations in oxygen fugacity and pH will cause uranium aqueous complexing to affect uranium solubility in the solution, as shown in figure 2. This phase equilibria diagram (figure 2) is a compilation of solution distribution calculations which shows variations in uranium mineral

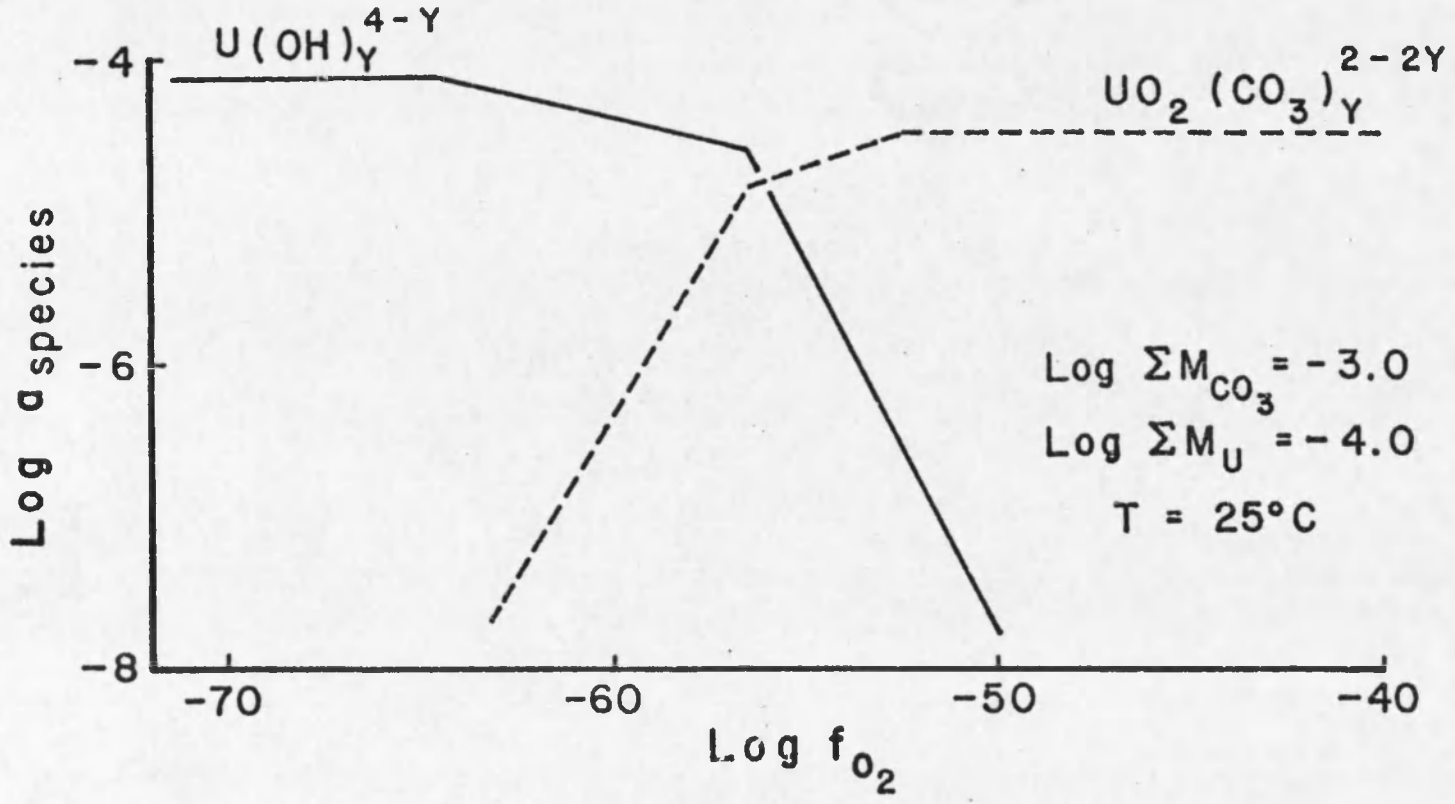

Figure 4. Log activity uranium aqueous species vs. log f_{O_2} for the dominant uranium complexes in a solution with log ΣM_U = -4.0, log ΣM_{CO_3} = -3.0, T = 25°C, P = 1 bar, a_{H_2O} = 1, and I = 0.1 molal.

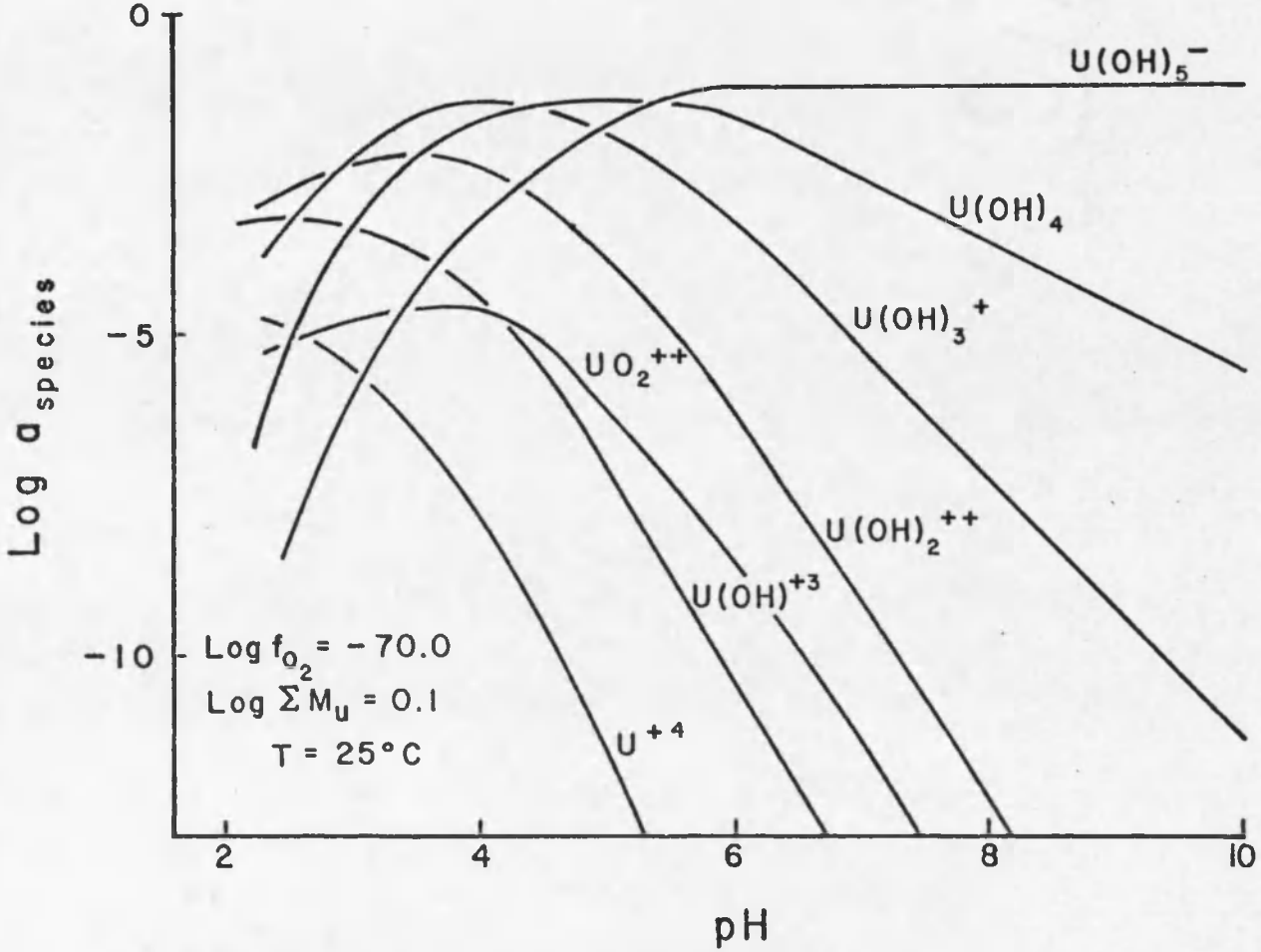

Figure 5. Log activity uranium aqueous species vs. pH depicting relative stabilities of uranium hydroxide species in a solution with log f_{O_2} = -70.0, log ΣM_U = 0.1, log ΣM_{CO_3} = 0.0, T = 25°C, P = 1 bar, a_{H_2O} = 1, and I = 0.1 molal.

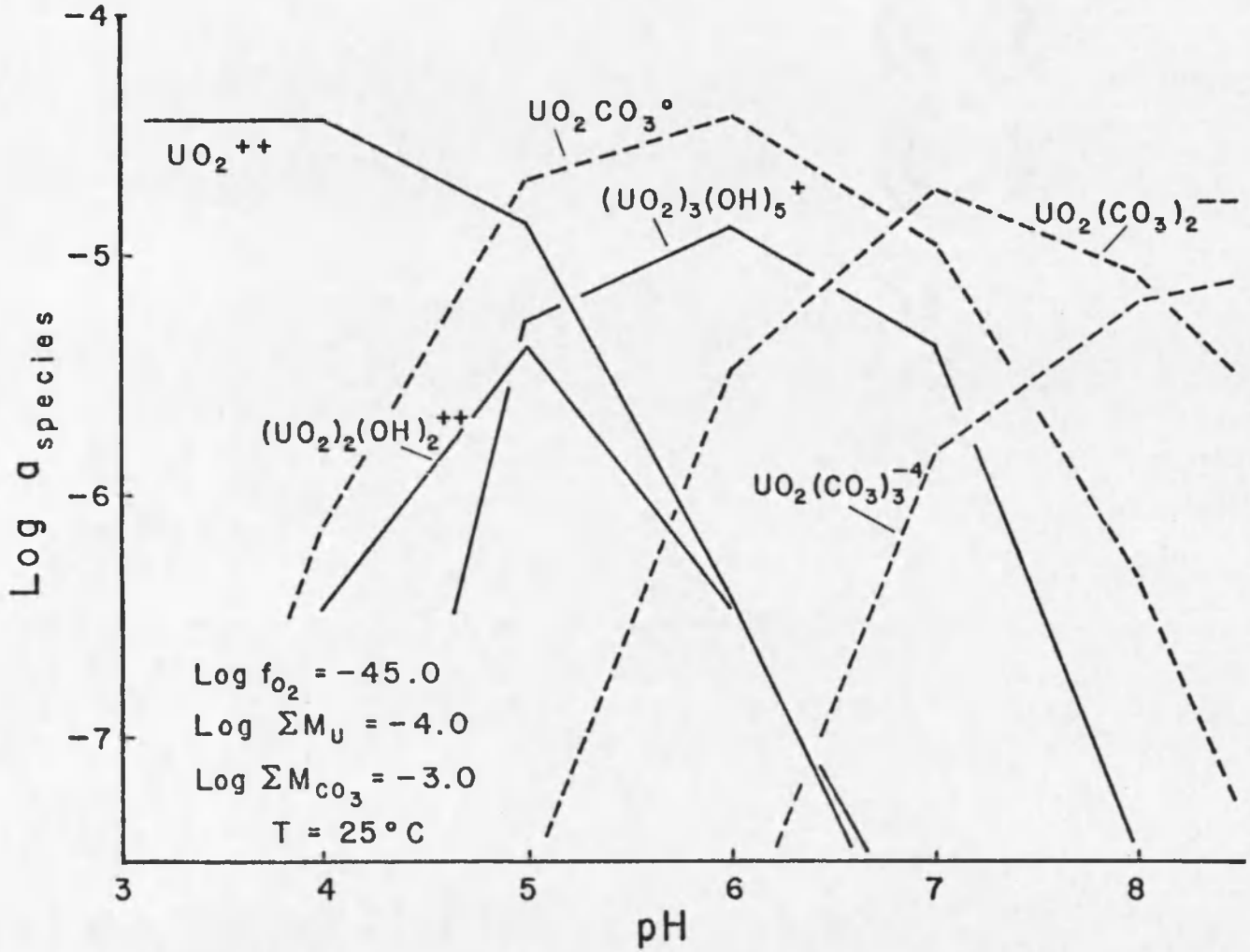

Figure 6. Log activity uranium aqueous species vs. pH depicting relative stabilities of uranium species in solution with log f_{O_2} = -45.0, log ΣM_U = -4.0, log ΣM_{CO_3} = -3.0, T = 25°C, P = 1 bar, a_{H_2O} = 1, and I = 0.1 molal.

equilibria with changing oxygen fugacity and pH. Solution-mineral equilibrium surfaces for pHs ranging from 6 to 9 are indicated by the solid lines. $UO_2(OH)_2$ is the stable phase that occurs in equilibrium with the oxidized solution, log $f_{O_2} > -45$, while UO_2 (uraninite) is the stable phase in equilibrium with the reduced solution.

The maximum concentration of uranium that can be transported in this acid groundwater is $10^{-3.7}$ molal at pH = 9 to $10^{-4.2}$ molal at pH = 7; under oxidized conditions (log $f_{O_2} > -45$), as shown in figure 2. In this environment total uranium is independent of oxygen fugacity because the stable phase in this region, $UO_2(OH)_{2(c)}$, contains U (VI), and the dominant species in this solution is a uranium (VI) carbonate:

$$UO_2(OH)_{2(c)} + (2-x)H^+ + xHCO_3^= \rightleftarrows UO_2(CO_3)_x^{2-2x} + 2H_2O. \quad (5)$$

The trend in this solution is for a decrease in pH to produce a reduction in uranium solubility. This trend is reversed in an oxidized solution, with log $f_{O_2} > -46$, at pH's > 7, because of the increasing importance of the uranium (VI) hydroxide species, $(UO_2)_3(OH)_5^+$, over the carbonate species in the more acidic solutions.

As oxygen fugacity decreases by 2 log units, in the range of log $f_{O_2} = -45$ to approximately -57, total uranium

in solution decreases by approximately a log unit (figure 2). This occurs because the stable phase in this region is uraninite, which contains uranium in the reduced state, while the dominant species in solution is a uranium (VI) carbonate, as shown in equation 6.

$$UO_{2(c)} + (2-x)H^{+} + 0.5\ O_{2(g)} + xHCO_3^{=} \rightleftarrows H_2O + UO_2(CO_3)_x^{2-2x} \qquad (6)$$

In this range of oxygen fugacities; a pH decrease of 1 unit will decrease maximum uranium in solution by .7 to .4 log units, depending on the initial pH (figure 2).

With continued decrease in oxygen fugacity, log $f_{O_2} < -57$, total uranium in solution is dependent on pH alone, resulting from increased importance of the reduced uranium hydroxide species, $U(OH)_5^{-}$, over the oxidized uranium carbonate species:

$$UO_{2(c)} + 3H_2O \rightleftarrows U(OH)_5^{-} + H^{+}. \qquad (7)$$

In this f_{O_2} range a pH decrease of 1 will decrease uranium solubility by 1 log unit.

Bicarbonate Groundwater

Solution-mineral equilibrium for a high carbonate groundwater that contains 10^{-1} molal total carbonate, with

a pH ranging from 7 to 9, was studied by the same methods as were used for examination of the acid groundwaters. The major difference between these two solutions, as can be seen through a comparison of figures 2 and 3, is that the increased importance of the uranium (VI) carbonate species allows the high carbonate groundwater to transport higher concentrations of uranium than does the lower carbonate acidic groundwater.

A maximum of $10^{-1.5}$ molal uranium can be transported in this carbonate solution; under oxidizing conditions, log $f_{O_2} > -45$. As in the acid groundwater, total uranium is independent of f_{O_2} because the uranium (VI) carbonate and uranium (VI) hydroxide species dominate. Below log $f_{O_2} = -45.$, uraninite becomes the equilibrium phase. In this region the uranium (VI) carbonate species continue to dominate the solution, and a decrease in oxygen fugacity of 2 log units requires the uranium concentration (log ΣM_U) to decrease by 1. Also, in this compositional region, a decrease from pH = 9 to 8 will decrease uranium concentration in solution by .65 log units, and a decrease in pH from 8 to 7 will produce a decrease of 1.20 log units in total uranium in solution. This pattern of reduction of maximum total uranium in solution with change in oxidation and pH will continue until log f_{O_2} decreases below -69. At this point the uranium (VI)

hydroxide species, $U(OH)_5^-$, becomes more important in the solution than the uranium (VI) carbonates, and pH alone will affect total uranium (figure 3).

Minerals

The equilibrium phases that limit total uranium concentrations, in the solutions studied, are $UO_{2(c)}$ and $UO_2(OH)_{2(c)}$. Coffinite, $U(SiO_4)_{1-x}(OH)_{4x}$, is also a possible precipitate from these solutions, depending on pH and the activity of silica in the solution, as shown in equation 8.

$$UO_2 + H_4SiO_4 \rightleftarrows U(SiO_4)_{1-x}(OH)_{4x} + 4xH^+ + (2-4x)H_2O \quad (8)$$

Coffinite stability, with respect to uraninite, increases with an increase in pH or activity of H_4SiO_4. Calculations based on the available data, which are for the dehydrated form, $USiO_4$, indicate that coffinite rather than uraninite would precipitate if the activity of silica in solution exceeded $10^{-2.9}$. This value of $10^{-2.9}$ would change with pH for the naturally occurring hydrated form.

NUMERICAL SIMULATION OF ORE FORMATION

Mineral zoning characteristics of a Wyoming roll-type uranium deposit could be formed as (1) an aerated acidic groundwater circulates into and reacts with the pyrite, biotite, quartz, feldspar, and calcite within a more reduced zone of the sandstone or (2) a carbonate groundwater (log $\Sigma M_{CO_3} > -1$), near equilibrium with the pyrite-bearing sandstone in which it is contained, either circulates into and reacts with a clay and hematite-bearing sandstone or mixes with an acidic groundwater.

The formation of these deposits was studied by numerical simulation of the irreversible reactions between a kg packet of ore-forming solution and the rocks through which it circulates. The mass transfer reactions between solutions and reactant minerals, characteristic of the ore deposit environment, were calculated using a modification of the computer program PATH (Helgeson, 1968; Helgeson, Garrels, and MacKenzie, 1969; Helgeson et al., 1970; and Knight, 1976). The extent to which minerals are produced or destroyed as a function of reaction progress is calculated by simultaneous solution of the differential equations describing the conservation of mass, the conservation of charge, and the reversible mass transfer in the system.

These calculations assume that (1) homogeneous equilibrium prevails among species in the aqueous solution, (2) heterogeneous equilibrium exists between solution and solid phases, (3) no mass is exchanged between the system and its surroundings, and (4) the activities of the solid phases and H_2O are unity.

Variations in the composition of the solution packet are defined by the extent of reaction with the host rocks. The effect of continued solution movement along its flow path is approximated by an open system calculation in which product phases are removed from the system as they form, thereby making reaction progress proportional to distance along the flow path.

Aerated Acidic Groundwaters Reacting with a Pyrite-Bearing Arkosic Sandstone

Infiltration of a packet of rainwater into an arkose containing biotite, quartz, feldspar, and calcite produces a compositional shift in the solution toward equilibrium with these minerals. Chemical changes which result from the reaction of this fluid packet with the sandstone are an increase in the concentration of ions in solution, a decrease of f_{O_2}, and an increase in pH, caused by the dissolution of the feldspars and biotite. The concentration of uranium in this solution is increased by dissolution of uranium from

the sediments. The groundwater produced by these reactions is of the type that has been proposed in the literature as a solution capable of forming uranium ore deposits. Calculations, in this study, indicate that flow of this solution into a more reduced zone in the sandstone produces a mineral zoning sequence similar to that associated with Wyoming roll-type deposits, and, if the concentration of uranium in solution is high enough, a uranium ore deposit will form.

First, the composition of this proposed ore-forming solution, an acidic groundwater, was estimated by simulation of the reactions between rainwater and the biotite, quartz, feldspar, and calcite cement that typically compose the sandstones surrounding these ore bodies. Initial compositions of the rainwater and arkosic sandstone are given in tables 6 and 7, respectively. Relative reaction rates for the reactant minerals are listed in table 7 and were calculated from the kinetic data in table 5 and the reactant surface areas given in table 7. Reactant surface areas for quartz, biotite, and the feldspars were calculated assuming a grain size of .03 cm and 15 percent porosity for the sandstone. Calcite's surface area was calculated, assuming it occurs as coatings on the sand grains (of less than .1 mm). The rate of depletion of dissolved oxygen from the solution was estimated for the rate of oxygen consumption by the

Table 6. Initial Compositions of the Rainwater and Aerated Arkosic Groundwater

	Rain[1]	Aerated Groundwater
Temp.	25°C	25°C
log f_{O_2}	-25.[2]	-30.
log f_{CO_2}	-1.5[3]	-1.7
pH	4.4[4]	6.0
i	Log ΣM_i	
Al	-10.0	-9.6
K	- 5.2	-3.6
Na	- 4.7	-4.5
Ca	- 4.7	-2.7
Mg	- 5.0	-5.1
Fe	-11.9	-12.9
Si	- 4.2	-3.1
S	- 4.7	-4.7
C	- 3.0[3]	-3.0
Cl	- 4.1	-2.4
U	-	-7.0
Dissolved O_{2_g}	- 2.9[5]	-5.8

[1]Rain composition taken from Garrels and MacKenzie (1971) and Sugawara (1967).

[2]Baas Becking, Kaplan, and Moore (1960).

[3]f_{CO_2} and total carbonate for rain in contact with soil horizon, Paces (1972).

[4]Calculated pH for rain after increase in f_{CO_2} due to interaction with soil horizon.

[5]Berner, 1971, p. 118.

Table 7. Composition of the Sandstone and Relative Reaction Rates of the Minerals

Phase	Arkose	Arkose with Pyrite	Log K_{25^oC}	Volumetric Surface Area	Relative Reaction Rates
	wt%	wt%	$g/cm^2 sec$	cm^2/cm^3 fluid	
Quartz	49	47	-20.4	13.3	-
K-Feldspar	44	44	-10.8	12.0	.18
Albite	2.5	2.5	-10.8	.7	.01
Anorthite	2.5	2.5	-10.8	.7	.01
Biotite Fe	.9	.9	- 9.6	$.2 \times 10^{-2}$	$.55 \times 10^{-4}$
Mg	.1	.1	- 9.6	$.2 \times 10^{-3}$	$.5 \times 10^{-5}$
Calcite	1	1	- 5.1	1.8	.04
Pyrite		2			.01[a]
Dissolved $O_{2(g)}$					$.1 \times 10^{-4}$[b] to .03[c]

[a]Extimation based on relative abundance in the rock.

[b]Estimation based on the rate of oxygen consumption by the reactant biotite.

[c]Estimation based on the rate of oxygen consumption by the reactants biotite and pyrite.

reactant mineral biotite. The acidic groundwater derived from the above mentioned reactions (composition listed in table 6) is in equilibrium with Ca-montmorillonite and hematite, is supersaturated with respect to quartz, still has minor concentrations of dissolved oxygen, and contains 10^{-7} molal (24. ppb) uranium.

The amount of uranium in this solution is consistent with uraninite kinetic data (Grandstaff, 1976), listed in table 5, which indicates that 10^{-7} molal uranium could be accumulated in approximately three days by an oxidized groundwater (log ΣM_{CO_3} = -3.0, pH = 5.5) flowing through an arkose, with 15 percent porosity and 10 ppm uraninite (uraninite reactant surface area is 10^{-5} cm^2 per cm^3 of fluid). Also, Sato's (1960) work on the oxygen content of mine waters indicates that groundwater maintains some dissolved oxygen until it comes into contact with oxygen-depleting minerals. Supersaturation with respect to quartz is consistent with the observation that silica solubility, at low temperatures, is controlled by amorphous silica (Siever, 1957).

Next, reactions between the ore-forming solution, derived from the above considerations, and the ore environment, composed of pyrite, biotite, quartz, feldspar, and calcite, were calculated for a rock composition and for

mineral reaction rates, summarized in table 7. As a packet of this acid groundwater flows into this reduced sandstone environment, the net effect is a decrease in the oxygen fugacity and an increase in pH of the solution, as shown in figure 7.

As the packet of 1 kg of acidic groundwater, initially in equilibrium with hematite and Ca-montmorillonite and with log f_{O_2} = -30.0, log f_{CO_2} = -1.5, pH = 6.0, and log ΣM_U = -7.0, flows through and reacts with the sandstone, f_{O_2} decreases but pH and f_{CO_2} do not, as shown in figure 7, zone 1. Decrease in f_{O_2} is caused by the dissolution of pyrite and biotite. pH remains constant, because the net decrease in hydrogen ion produced by the dissolution of the feldspars is both replenished by the precipitation of Ca-montmorillonite and is partially buffered by the carbonate complexes.

As a result of this decrease in f_{O_2}, brought about by the continued reaction between this packet of acidic groundwater and the sandstone, a sequence of mineral products forms, as shown in figure 8. The first precipitate is uraninite, which equilibrates with the solution at log f_{O_2} = -49.5, as shown in figure 2, point A. As uraninite precipitates, carbonate is released from the uranium carbonate complexes, but, as can be seen in figure 9, it is in such

Figure 7. Log f_{O_2}, log f_{CO_2}, pH as a function of log reaction progress for reactions between acid groundwaters and a pyrite-bearing arkose.

Chemical evolution of the solution, depicted on the lower part of the figure, is divided into three distinct zones, shown at the top. Minerals in equilibrium with the solution are indicated by solid lines representing mineral precipitation and dashed lines representing reversible dissolution.

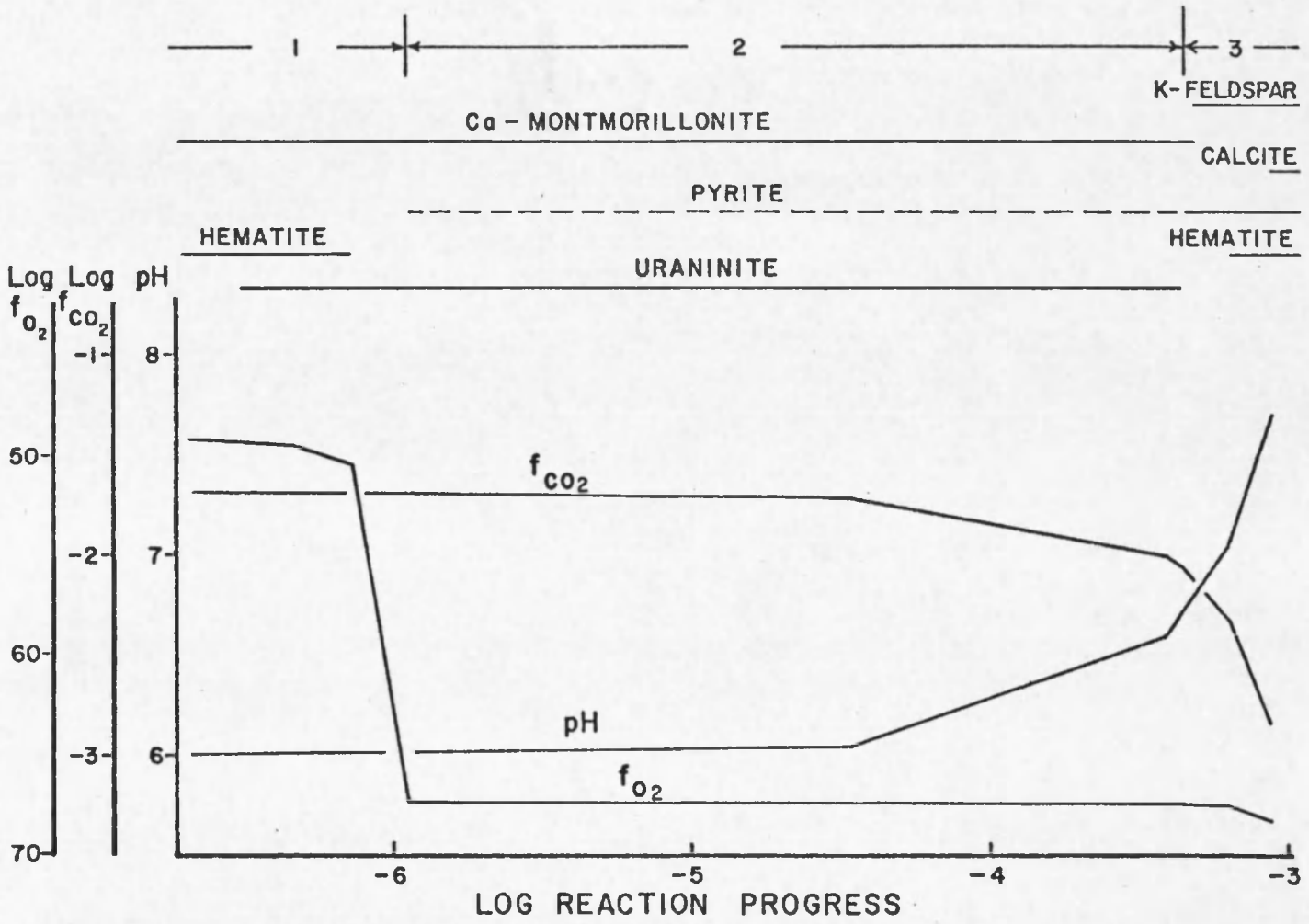

Figure 7. Log f_{O_2}, log f_{CO_2}, pH as a function of log reaction progress for reactions between acid groundwaters and a pyrite-bearing arkose.

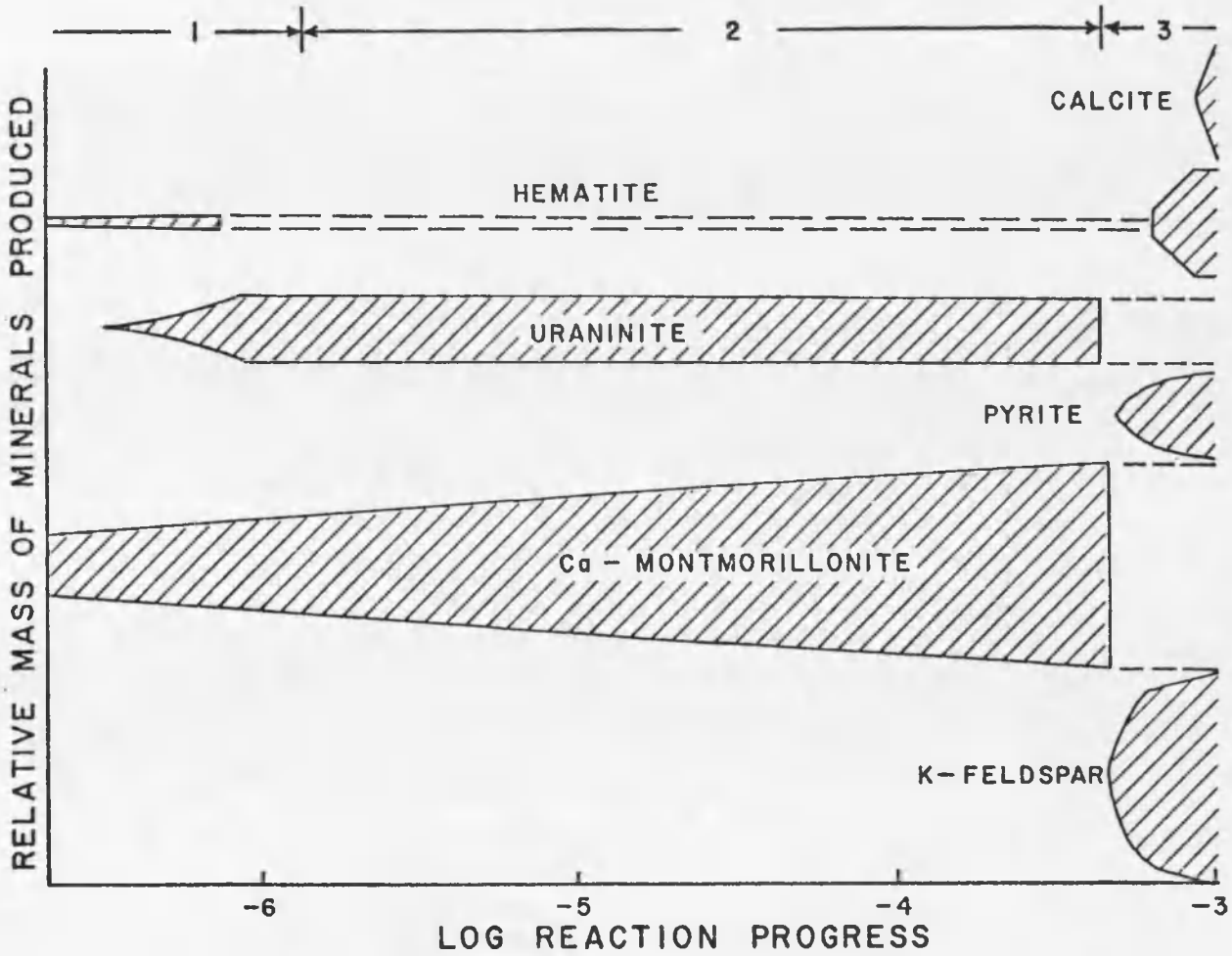

Figure 8. Relative mass of mineral produced as a function of reaction progress for reactions between acid groundwaters and a pyrite-bearing arkose.

The chemical evolution of the solutions is divided into three zones, which are indicated at the top of the figure.

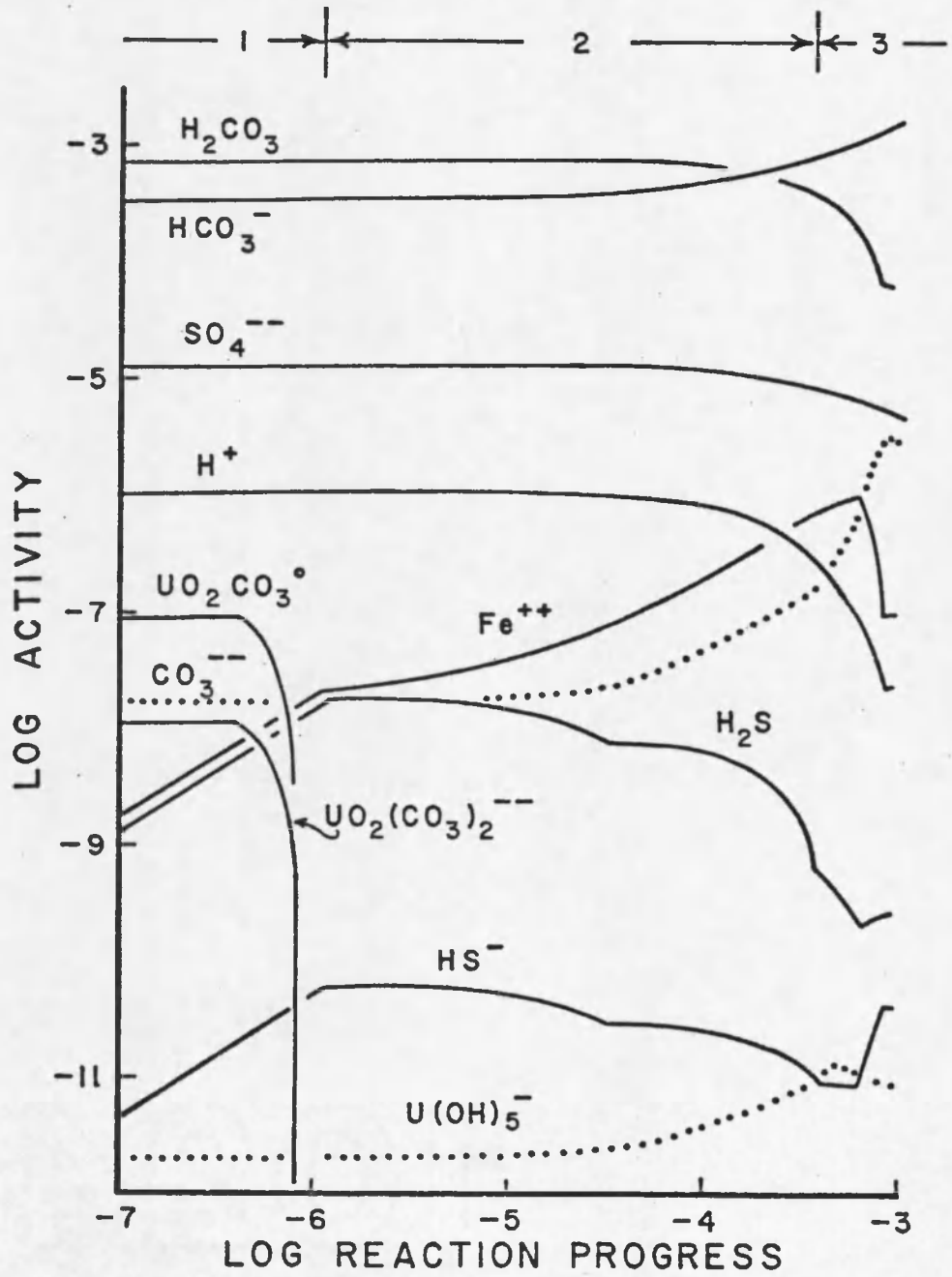

Figure 9. Log activity vs. log reaction progress of aqueous species relevant to the discussion of the reactions between groundwaters and a pyrite-bearing arkose.

The chemical evolution of the solution is divided into three zones, which are indicated at the top of the figure.

small quantities that it has no affect on the total carbonate in solution. Reduction of the fluid packet to log f_{O_2} = -56.6 consumes all the dissolved oxygen in the solution, at which point the solution composition shifts away from hematite equilibrium. This is a result of the net decrease in Fe^{+3}, in spite of the increase in total iron from the irreversible dissolution of pyrite and biotite. Next, pyrite will equilibrate with the solution at log f_{O_2} = -67.4 but will continue to dissolve, producing a change in the style of compositional variation with further reaction progress.

Uraninite and Ca-montmorillonite precipitation from the groundwater, with concomitant pyrite dissolution, buffers the oxygen fugacity, causing pH to increase and f_{CO_2} to decrease with continued reaction progress (figure 7, zone 2). Pyrite dissolution is a consequence of two factors: (1) the increasing pH, brought about by the dissolution of the feldspars, and (2) the oxidizing effect of the conversion of oxidized uranium (VI) carbonate species to reduced uranium (IV) for uraninite precipitation. Increasing f_{CO_2} with these reactions is in response to the hydrogen ion decrease which produces a decrease in the concentration of H_2CO_3 with respect to HCO_3^- and $CO_3^=$. The pH decrease, with continued flow and reaction of the packet of groundwater with the sandstone, will shift the solution composition away from

uraninite equilibrium, at log f_{O_2} = -67.4, pH = 6.7, log f_{CO_2} = -2.0, and log ΣM_U = -11.0, as shown on figure 2, point B. This shift from uraninite equilibrium is a result of the increased importance of the dominant uranium complex in this solution, $U(OH)_5^-$, with increasing pH, shown in figure 9, zone 2.

With further influx of the fluid packet and reaction with the sandstone, pyrite will begin to precipitate as a result of the decreasing f_{O_2} caused by biotite dissolution. Figure 7, zone 3, indicates that f_{O_2} again decreases while pH increases and f_{CO_2} decreases with reaction progress. The decreasing hydrogen ions, in conjunction with the increase in potassium from the dissolution of the feldspars, shift the silicate equilibrium in the fluid packet from Ca-montmorillonite to K-feldspar (figure 10) at log f_{O_2} = -67.4, pH = 6.7, and log f_{CO_2} = -2.0 (figure 7). This decrease in the concentration of hydrogen ions, along with the small change in f_{O_2}, will shift the solution composition back to hematite equilibrium at log f_{O_2} = -67.6, pH = 7.1, and log f_{CO_2} = -2.3 (figure 7). Continued reaction of this packet of groundwater as it flows through the host rocks will finally shift its composition into the calcite stability field at log f_{O_2} = -68.2, pH = 7.7, and log f_{CO_2} = -2.9 (figures 7 and 10). With continued reaction progress, the

Figure 10. Activity-activity diagram depicting the reaction path between the acid groundwater and sandstone at 25°C, 1 bar $a_{solids} = 1$, and $a_{H_2O} = 1$.

The system is UO_2-UO_3-CaO-K_2O-Al_2O_3-SiO_2-SO_4-H_2S-CO_2-H_2O. Circles represent the following phase boundaries:

A - Starting solution and initial uraninite saturation at log $f_{O_2} = -49.6$ and pH = 6.0;

B - Hematite out of equilibrium at log $f_{O_2} = -50.6$ and pH = 6.0;

C - Pyrite equilibrium at log $f_{O_2} = -67.4$ and pH = 6.0;

D - Uraninite out of equilibrium at log $f_{O_2} = -67.4$ and pH = 6.7;

E - Silicate equilibria shifts from Ca-montmorillonite to K-feldspar at log $a_{H_4SiO_4} = -2.9$, pH = 6.8, and log $a_{K^+}/a_{H^+} = 3.55$;

F - Hematite equilibrium at log $f_{O_2} = -67.6$ and pH = 7.1;

G - Calcite saturation at log $f_{CO_2} = -2.8$ and pH = 7.7.

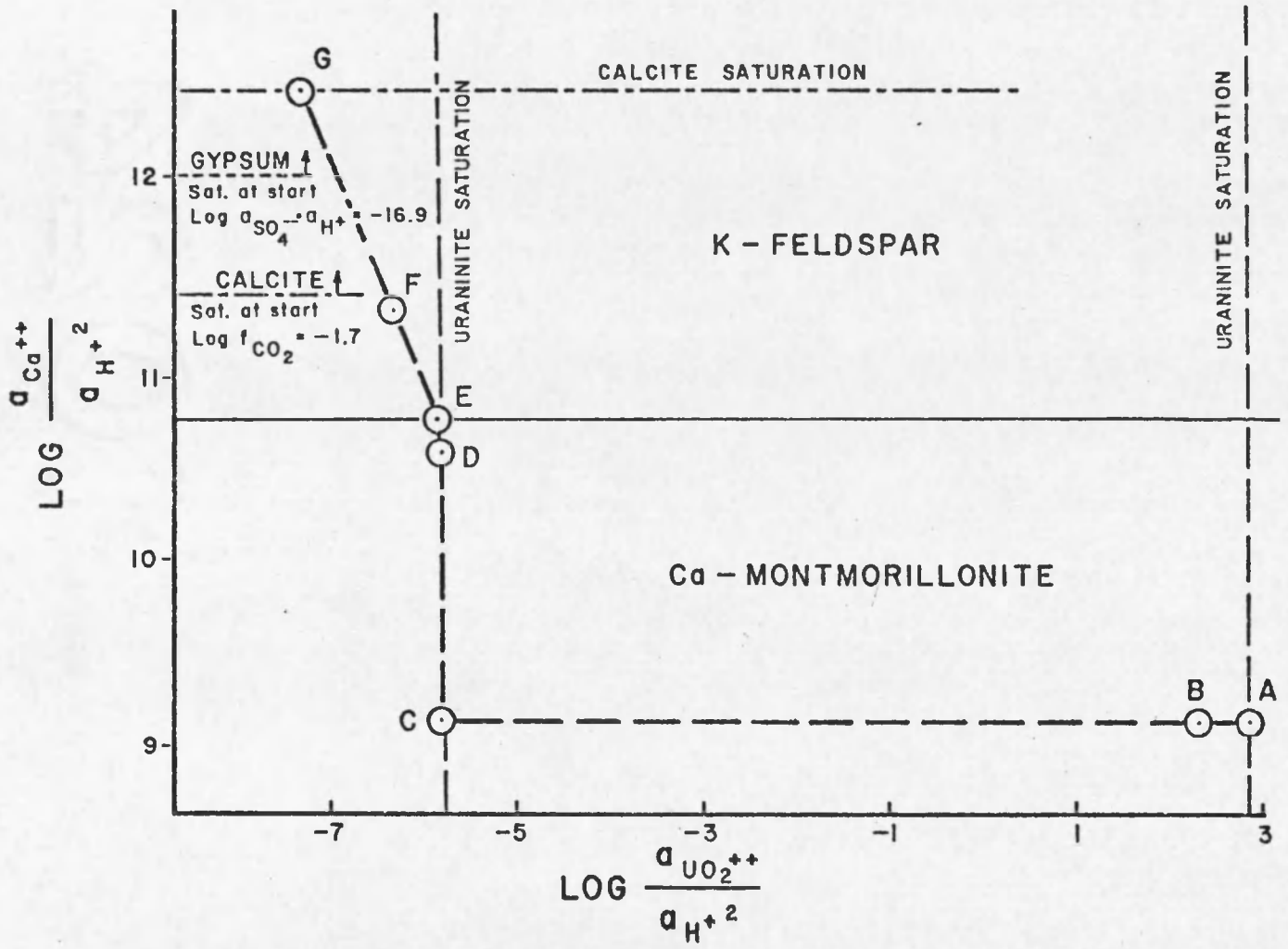

Figure 10. Activity-activity diagram depicting the reaction path between the acid groundwater and sandstone at 25°C, 1 bar, $a_{solids} = 1$, and $a_{H_2O} = 1$.

chemical composition of the fluid packet will ultimately shift into overall equilibrium with the reactant phases and final produce minerals.

This groundwater which transports 10^{-7} molal uranium (24. ppb) will initially precipitate 2.7×10^{-5} grams of uraninite per kg of solution influx. With continued influx of fluid packets into the sandstone aquifer, an ore grade deposit will eventually be concentrated. As the acid groundwater, carrying 10^{-7} molal uranium, flows through the sandstone aquifer (which has a density of 2.6 g/cm^3), it will concentrate .25 percent UO_2 into a 4 m wide ore body, after 96,000 kg of solution influx. With a constant flow rate of 10^{-3} cm^3/sec in the aquifer, it would take approximately 3,000 years to concentrate this ore body. If this acidic ore-forming solution had concentrated only 10^{-8} molal urainium (2.4 ppb), uraninite would have precipitated at a lower f_{O_2}, of 10^{-52} (as shown in figure 2), than for the higher uranium solution. A solution of this composition would precipitate 2.7×10^{-6} grams of uraninite per kg of solution and would take approximately 30,000 years to concentrate a .25 percent UO_2, 4m wide ore body, as discussed above.

The masses of other minerals produced or destroyed per kg of solution influx are listed in table 8, and the

Table 8. Total Mass of Minerals Produced and Destroyed per kg of Acidic Groundwater Reacted to Calcite Equilibrium

Mineral	Mass Produced (g)	Mass Destroyed (g)
K-Feldspar	5.02×10^{-2}	9.90×10^{-2}
Albite		2.12×10^{-2}
Anorthite		2.24×10^{-2}
Biotite Fe		2.27×10^{-4}
Mg	1.11×10^{-3}	9.46×10^{-6}
Pyrite	5.20×10^{-5}	8.85×10^{-5}
Hematite	1.19×10^{-4}	
Calcite		3.23×10^{-2}
Ca-montmorillonite	6.53×10^{-2}	
Uraninite	2.70×10^{-5}	
Dissolved $O_{2(g)}$		$.16 \times 10^{-5}$

relative masses of minerals produced with reaction progress are shown in figure 8. Reaction progress is relative to distance along the solution flow path; therefore, figure 8 represents the sequence of mineral deposition within the ore deposit, with the altered sandstone on the left and the unaltered sandstone on the right. The vertical axis on figure 8 is proportional to the mass of mineral produced. Calculations indicate, as shown on figure 8, zone 1, that when uraninite initially equilibrates with the solution the greatest concentration is precipitated at the contact with the altered sandstone. There is also a gap, containing minor amounts of uranium, between this uranium-rich zone and the region where the most pyrite is precipitated. Pyrite also deposits in the largest quantity with initial precipitation and tapers off with continued solution flow (figure 8, zone 3). Ca-montmorillonite precipitates at an almost constant rate in the altered sandstone (figure 8, zones 1 and 2), until the solution shifts to K-feldspar equilibrium.

This calculated pattern of mineral precipitation in the ore zone is consistent with that characteristic of these ore bodies, such as (1) the occurrence of the greatest concentration of uranium at the contact with altered sandstone and (2) deposition of the major concentration of pyrite beyond this region of greatest uranium concentration and extending into unaltered sandstone.

Variations in the mineral zoning associated with each particular deposit may be a product of differences in composition of the ore-forming solutions and gangue minerals. In the same manner, differences between these predictions and mineral zoning seen in nature may also be a result of the selection of initial solution and reactant minerals. For example, these calculations indicate that hematite will precipitate from the acid groundwater in the altered sandstone while pyrite is reacting, only if there is dissolved oxygen present in the solution. Therefore, if dissolved oxygen is consumed before uraninite precipitation, a band of bleached sandstone, without hematite, forms on the altered side of the roll, as described by Granger and Warren (1974). These calculations do not account for the occurrence of unweathered euhedral pyrite grains found in this band in some localities (Granger and Warren, 1974).

In summary, the calculated mineral zoning sequence produced during the reaction of a uranium-bearing aerated acidic groundwater with a reduced region in the arkosic sandstone through which it flows is as follows: (1) A bleached zone in which the acidic oxidized solution dissolves calcite, pyrite, quartz, feldspar, and biotite and precipitates Ca-montmorillonite and hematite in the relative total concentrations shown in figure 8. (2) A uraninite

Ca-montmorillonite zone containing a band of hematite at the contact with zone 1. Dissolution of calcite, pyrite, quartz, feldspar, and biotite extends into this zone. (3) A zone containing pyrite with less alteration of the sandstone because K-feldspar, a major constituent of the sandstone, is in equilibrium with the solution and because the solution at this point of influx is reducing and nearly neutral. However, calcite cement has been leached from this zone. (4) Unaltered sandstone containing pyrite and hematite, but no calcite. (5) Unaltered sandstone containing pyrite, hematite, and calcite. (6) Barren unaltered calcite cemented sandstone.

Bicarbonate Groundwaters Reacting with Altered Host Rocks or Mixing with Acidic Groundwaters

If uranium is available in the sediments, it will concentrate during the formation of a high carbonate groundwater and through evaporation and reaction with the sediments. A comparison of figures 2 and 3 shows that high carbonate groundwater can transport orders of magnitude more uranium than the acidic groundwaters previously discussed. A zoning sequence similar to that associated with uranium roll-type deposits will form when this uranium-bearing high carbonate solution, near equilibrium with the minerals that typically compose the sandstone associated with these

deposits (pyrite, biotite, quartz, feldspar, and calcite), flows from this environment into a weathered zone in the sandstone. This zoning sequence would also be produced if acidic groundwaters infiltrated into the environment of the carbonate groundwater and mixed with them.

The concentrations of the major components in this proposed ore-forming solution are taken from Eugster's (1970, p. 211, table 2) measured composition of carbonate groundwater associated with a present-day carbonate evaporite lake environment. The actual solution composition used in these calculations (listed in table 9) is Eugster's groundwater composition modified as follows: (1) not supersaturated with any minerals except quartz, (2) in equilibrium with calcite and K-feldspar, and (3) near equilibrium with pyrite and biotite. This groundwater, then, represents a solution nearly in equilibrium with a pyritic arkose in which it is contained, having a carbonate concentration of $10^{-.52}$ molal with pH = 9 and $10^{-5.4}$ molal uranium.

Reactions between this ore-forming solution and the weathered sandstone environment are simulated by reacting a kg of carbonate groundwater (composition in table 9) with kaolinite and hematite (having relative reaction rates of 10:1, respectively). These calculations also simulate the effect of mixing acid groundwaters, present in the altered

Table 9. Composition of Bicarbonate Groundwater

f_{O_2}	-68.0
f_{CO_2}	- 2.1
pH	9.0
i	Log ΣM_i
Al	- 9.40
K	- 1.30
Na	- .06
Ca	- 4.91
Mg	-10.00
S	- .70
Si	- 3.52
Fe	- 9.00
C	- .52
Cl	- .97
U	- 5.36

sandstone, with the carbonate groundwaters found in the arkosic sandstones of the basin.

As a packet of carbonate groundwater, initially in equilibrium with calcite and K-feldspar, with log f_{O_2} = -68.1, log f_{CO_2} = -2.1, pH = 9.0, and log ΣM_U = -5.4, flows through and reacts with the altered sandstone, it will initially undergo a decrease in f_{O_2} with no change in pH or f_{CO_2} (figure 11, zone 1). The constant pH associated with this reaction is a result of the net increase in hydrogen ions being buffered by both an increase in HS^-, at the expense of $SO_4^=$, and an increase in HCO_3^-, at the expense of $CO_3^=$. Decrease in f_{O_2} is a result of conversion of $SO_4^=$ to HS^-, an effect which is greater than the oxidizing effect of hematite dissolution (figure 12; the change in $SO_4^=$ is too small to be apparent on this figure). The decrease in $CO_3^=$, as HCO_3^- increases, causes the solution to undersaturate with calcite, although it is not a large enough change to affect f_{CO_2} (this change is also not apparent on figure 12).

The sequence of mineral products formed as a result of the continued reaction of this packet of groundwater with the altered sandstone is shown in figure 13. Pyrite equilibrates with the groundwater at log f_{O_2} = -68.0, in response to both the decrease in f_{O_2} and the increase in iron concentration in solution as a result of hematite dissolution.

Figure 11. Log f_{O_2}, log f_{CO_2}, pH as a function of log reaction progress for reactions between bicarbonate groundwaters and altered sandstone.

Chemical evolution of the solution, depicted in the lower part of this figure, is divided into three distinct zones, shown at the top. Minerals in equilibrium with the solution are indicated by solid lines representing mineral precipitation and dashed lines representing reversible dissolution.

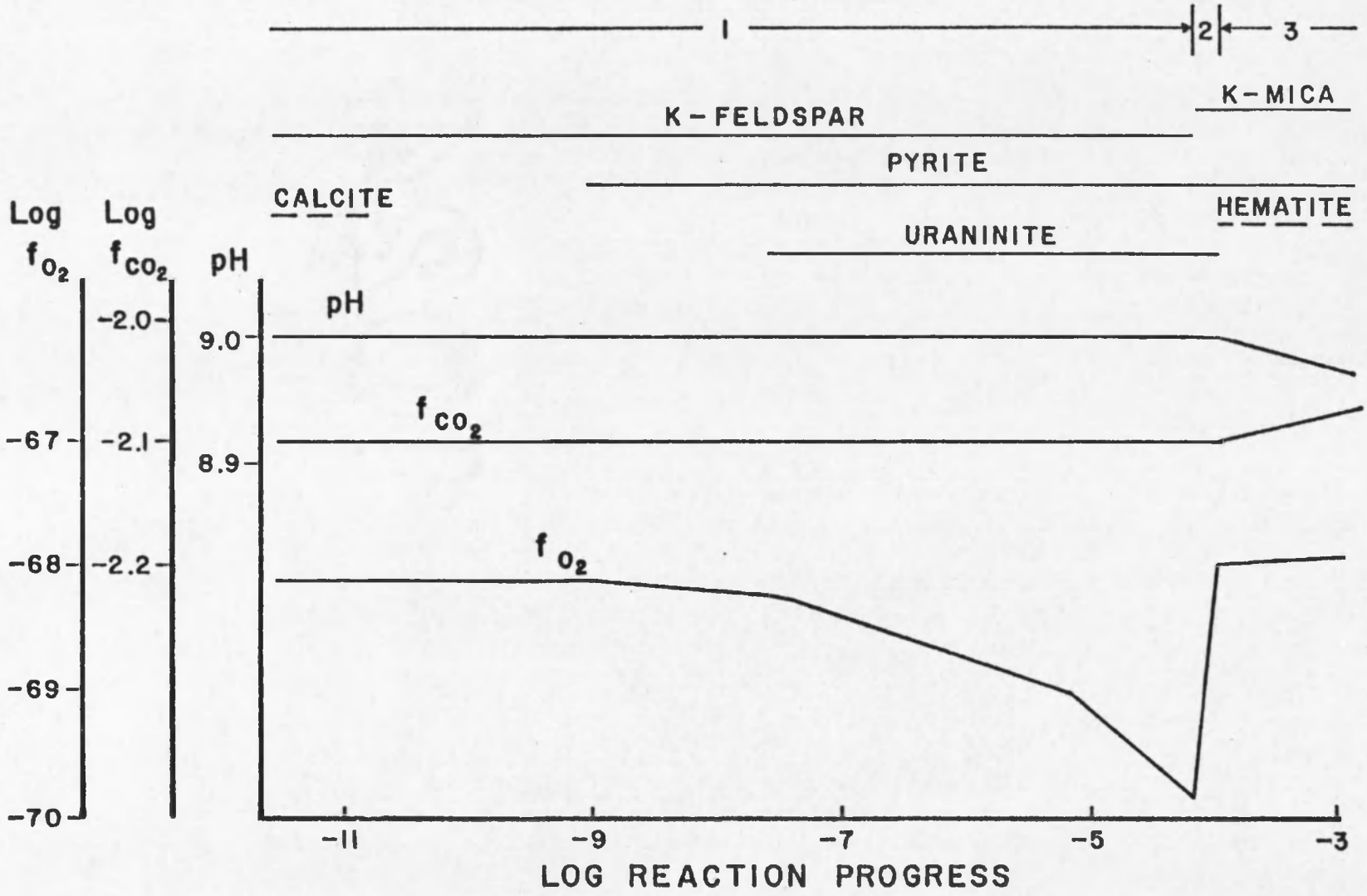

Figure 11. Log f_{O_2}, log f_{CO_2}, pH as a function of log reaction progress for reactions between bicarbonate groundwaters and altered sandstone.

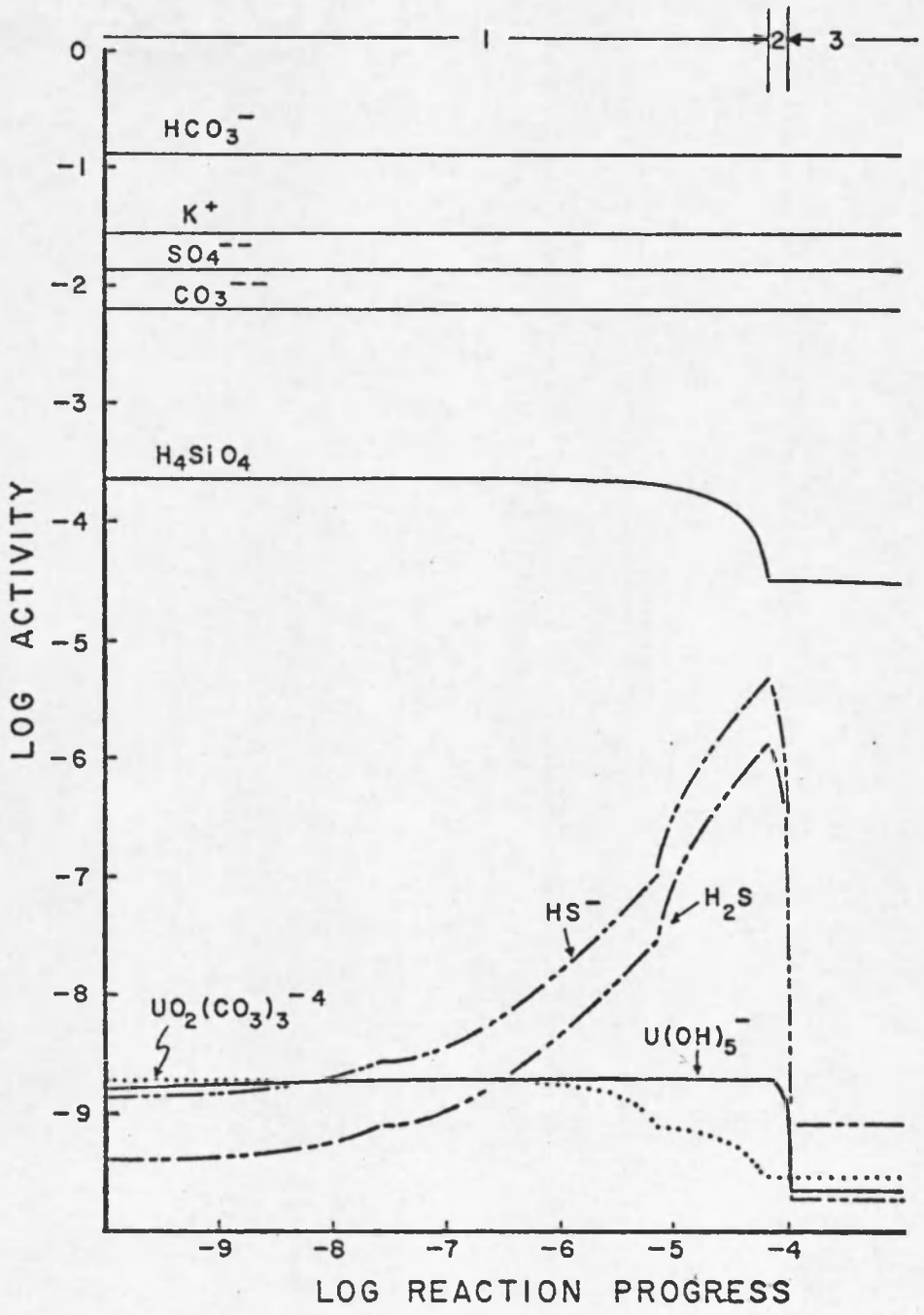

Figure 12. Log activity vs. log reaction progress of aqueous species relevant to the discussion of the reactions between bicarbonate groundwaters and altered sandstone.

The chemical evolution of the solution is divided into three zones, which are indicated at the top of the figure.

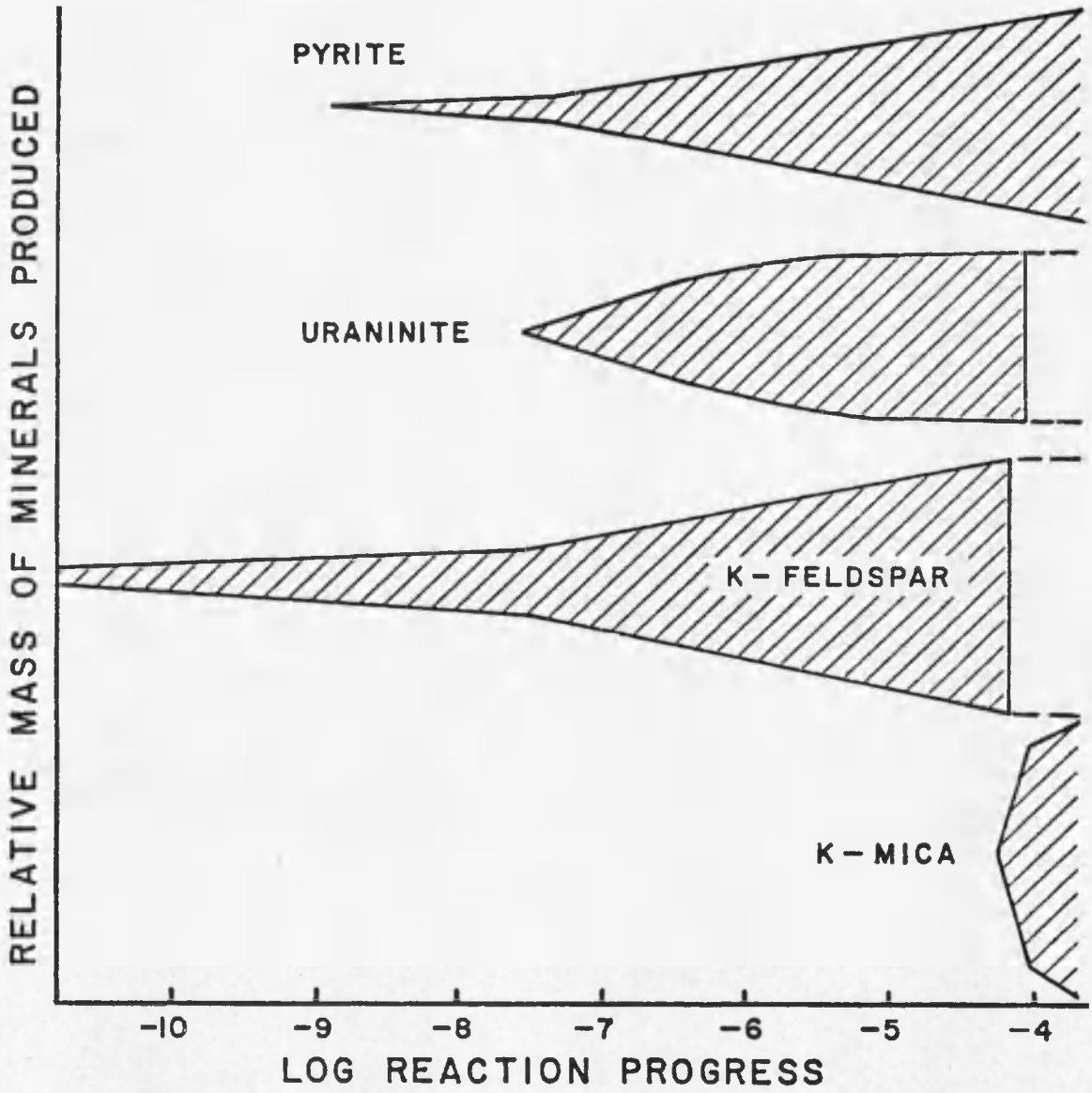

Figure 13. Relative mass of mineral produced as a function of reaction progress for the reactions between bicarbonate groundwaters and altered sandstone.

The f_{O_2} decrease will also shift the solution to uraninite equilibria at log f_{O_2} = -68.3, caused by a decrease in the oxidized uranium (VI) carbonate species, as shown in figure 12.

K-feldspar precipitates with continued solution flow and reaction progress and causes a decrease in potassium and silica concentrations in the solution (figure 12), eventually resulting in a shift in silicate equilibria from K-feldspar to K-mica, at log f_{O_2} = -69.9, log f_{CO_2} = -2.1, and pH = 9. With K-mica precipitation, oxygen fugacity will begin to increase rather than decrease as before, again with no affect on pH or f_{CO_2}.

This increase in f_{O_2}, with continued reaction between the packet of groundwater and the altered sandstone, is a result of: (1) a decrease in the net increase of hydrogen ions caused by kaolinite dissolution, thereby reducing the effect of HS^- complexing on f_{O_2}. This change in the rate of hydrogen ion increase is a result of K-mica precipitation rather than K-feldspar precipitation as in previous reactions. (2) the oxidizing effect of hematite dissolution, and (3) continued pyrite precipitation, as a result of increasing total iron through hematite dissolution. Pyrite precipitation depletes the solution of sulfate and sulfide ions, but, because sulfide is orders of magnitude less than

the sulfate concentrations, there is a marked decrease in sulfide, while the concentration of sulfate changes only slightly.

The effect of this increase in oxygen fugacity on the mineral zoning produced is shown in figure 13. Initially, the solution will shift its equilibria away from uraninite at log f_{O_2} = -69.8, resulting from an increase in the uranium (VI) carbonate species. Next, hematite will equilibrate with the solution at log f_{O_2} = -68.0. Hematite continues to dissolve, and, in conjunction with kaolinite dissolution, pyrite and K-mica precipitation, pH will begin to decrease while f_{O_2} continues to increase, but at a much slower rate than before (figure 11, zone 3).

This high carbonate groundwater transporting $10^{-5.4}$ molal uranium (.9 ppm) will precipitate 1 x 10^{-3} grams of uraninite per kg of solution flowing through the rock. Continued flow of uranium-bearing groundwaters into the altered sandstone would eventually concentrate an ore grade deposit. It would take 2,600 kg of solution influx into this altered sandstone (having a density of 2.6 g/cm^3) to produce a 4 km wide, 0.25 percent UO_2, ore deposit. With a constant flow rate of 10^{-5} cm^3/sec for the groundwater passing into the altered sandstone, it would take approximately 8,200 years to concentrate this ore body.

The masses of other minerals produced or destroyed per kg of solution influx are listed in table 10, and the relative masses of minerals produced with reaction progress are shown in figure 13. Figure 13 (similar to the previously discussed figure 8) represents the predicted sequence of mineral deposition within the deposit, with the altered sandstone on the right and the unaltered sandstone on the left. Pyrite deposition extends beyond the uraninite ore zone on both sides into altered and unaltered ground (figure 13). Pyrite precipitates at nearly a constant rate, leaving almost the same concentrations in all regions where it is precipitated. Uraninite is precipitated in only minor concentrations at the contact with the altered sandstone, with major concentrations of uranium occurring a short distance into the unaltered sandstone. This is contrary to what is noted for uranium occurrences in nature, in which the uranium is concentrated at the contact with the barren altered sandstone. These calculations do show the occurrence of unweathered pyrite extending into the altered sandstone, and a zone of non-hematitic altered sandstone at the contact with the ore zone, as discussed by Granger and Warren (1974).

In summary, the zoning sequence produced when a uranium-bearing carbonate groundwater reacts with a weathered sandstone through which it flows, or mixes with an acid

Table 10. Total Mass of Minerals Produced and Destroyed per kg of Bicarbonate Groundwater Related to Hematite Equilibrium

Mineral	Mass Produced (g)	Mass Destroyed (g)
Pyrite	$.22 \times 10^{-2}$	
Hematite		$.15 \times 10^{-2}$
Uraninite	$.10 \times 10^{-2}$	
Kaolinite		$.24 \times 10^{-1}$
K-Feldspar	$.36 \times 10^{-1}$	
Muscovite	$.75 \times 10^{-2}$	

slightly more oxidized groundwater, is: (1) an alteration mineral zone in the sandstone containing pyrite, biotite, quartz, feldspar, and calcite cement, in which the carbonate groundwater is near equilibrium, (2) pyrite-bearing sandstone from which the calcite cement and pyrite were leached during initial weathering and from which the clays and hematite were dissolved by the ore-forming solution, (3) same as zone 2, with the addition of uraninite, (4) same as zone 2, with the addition of K-mica, and (5) altered sandstone containing hematite and clay minerals.

These calculations indicate that a uranium-bearing carbonate groundwater could be responsible for the formation of a zoning sequence that is characteristic of roll-type uranium deposits. These high carbonate ore-forming solutions will precipitate two orders of magnitude more uranium than an equivalent influx of acidic groundwater, thereby decreasing the amount of solution flow necessary for ore formation. A more concentrated carbonate brine solution could carry much higher amounts of uranium and could, thereby, precipitate greater quantities of uranium per kg of solution.

The origin for these high carbonate groundwaters would be the same mechanism responsible for the formation of the carbonate brine solutions from which the trona beds in the Eocene Green River Formation of southwestern Wyoming

precipitated. Eugster and Surdham (1973) suggested CO_2 charged groundwaters that react with igneous and metamorphic rocks as they flow into a closed basin under intense evaporitic conditions as the mechanism of carbonate brine formation in this Eocene basin. It is possible that the same mechanism operated in other areas of Wyoming during the Eocene to trap high carbonate groundwaters in the sediments. The source of weathered sandstone, in this discussion, would be a buried, ancient surface weathering zone.

If the ore formation is a result of carbonate groundwaters passing from their equilibrium environment by tilting or compaction, or other structural readjustments of the sediments, it is apparent that the shape of the deposit would be indistinct, as is true of many uranium occurrences, due to the slow rate of solution flow. For the same reason, a reverse roll would not be expected. If ore formation is a result of acidic groundwater infiltrating into and mixing with uranium-bearing carbonate groundwaters, then it is possible that the model crescent roll shape would be formed.

CONCLUSIONS

Two proposed mechanisms of uranium roll formation have been studied using thermochemical data and computations of irreversible mass transfer reactions. They are: (1) formation by an oxidized acidic groundwater infiltrating into a reduced zone in the sandstone through which it flows, a process currently popular in the literature, and (2) formation by a carbonate groundwater flowing into and reacting with an altered sandstone, or mixing with an acidic groundwater.

It is also apparent from this study that changes in the chemical character of the ore-forming solution across the mineralized zone are the same for both mechanisms, although the solution in the altered sandstone is oxidized and acidic, while in the unaltered solution it is reduced and basic. The major difference between these two modes of formation is the source region for uranium; the acidic oxidized groundwater leaches its uranium from the altered oxidized sediments, while the carbonate groundwater derives its uranium from sediments in the basin.

From this study it is evident that the mechanism of ore formation by an oxidized acid groundwater passing into a reduced zone in the sandstone is probably an ineffective

mechanism for transporting uranium over long distances in the subsurface environment. This is so because the oxidation potential of groundwaters changes rapidly from surface conditions of $f_{O_2} \sim -25.$ to $f_{O_2} \sim -65.$ as they react with pyrite and biotite in the sediments, thereby losing their ability to transport uranium. Less than 2×10^{-5} g of biotite and 3×10^{-6} g of pyrite would have to dissolve into a kg of rainwater to decrease its oxygen fugacity below the value 10^{-65}. At this f_{O_2}, acid groundwaters would not be able to transport significant concentrations of uranium (figure 2). Further reduction of this solution would not be a mechanism for ore formation, while a pH decrease would (figure 2), though this is unlikely at depth in a feldspar-rich environment. This indicates that reduction of acidic groundwaters would be an effective mechanism for uranium ore deposition over relatively short distances of solution influx from the surface.

Since reduced carbonate-rich groundwaters are possible ore-forming solutions, closed basins containing saline fluids, particularly if these solutions contain $\Sigma M_{CO_3} \sim 10^{-1}$, are possible exploration targets. This is based on the possibility of high enough amounts of uranium being concentrated in saline basin groundwaters for later deposition at the outer boundaries of the restricted basin environment.

From this study of the chemistry of this ore deposit environment, it is apparent that the reaction of solutions with rocks is important to uranium ore formation. Moreover, a more complete understanding of the mechanism of formation requires knowledge of the abundance and composition of minerals which occur in this environment, in particular the alteration of gangue minerals needs to be quantitatively defined. Further testing of these two hypotheses also requires an understanding of the precipitation mechanism of molybdenum, selenium, and other elements that occur as part of the zoning sequence. Such an expansion of this study would require a compilation of the thermochemical data for the minerals and aqueous species of these elements.

REFERENCES

Aagaard, P. and Helgeson, H. C., 1977, Thermodynamic and kinetic constraints on the dissolution of feldspars (abs.): Geol. Soc. Am., Abs. with Progs., v. 9, p. 873.

Adler, H. H., 1974, Concepts of uranium ore formation in reducing environments in sandstones and other sediments, in Formation of Uranium Ore Deposits: Internat. Atomic Energy Agency, Vienna, p. 141-168.

Adler, H. H. and Sharp, B. J., 1967, Uranium ore-rolls, occurrences, genesis, and physical and chemical characteristics: Utah Geol. Soc. Guidebook, no. 21, p. 53-77.

Ahrland, S., 1951, On the complex chemistry of the uranyl ion. V. The complexity of uranyl sulfate: Acta Chem. Scand., v. 5, p. 1151-1167.

Allen, K. A., 1958, The uranyl sulfate complexes from tri-n-octylamine extraction equilibria: Jour. Am. Chem. Soc., v. 80, p. 4133-4137.

Anderson, D. C., 1969, Uranium deposits of the Gas Hills: Contr. to Geol., Wyoming Univ., v. 8, no. 2, pt. 1, p. 93-103.

Armstrong, F. C., 1970, Geologic factors controlling uranium resources in the Gas Hills District, Wyoming: 22nd Ann. Field Conf., Wyoming Geol. Assoc. Guidebook, p. 31-44.

Austin, S. R., 1970, Some patterns of sulfur isotope distribution in uranium deposits: Wyoming Geol. Assoc. Earth Sci. Bull., v. 3, no. 2, p. 5-22.

Baas Becking, L. G. M., Kaplan, I. R., and Moore, D., 1960, Limits of the natural environment in terms of pH and oxidation potentials: Jour. Geol., v. 68, p. 243-284.

Baes, C. F., Jr. and Mesmer, R. E., 1976, The Hydrolysis of Cations: New York, John Wiley & Sons, 489 p.

Bailey, R. V., 1969, Uranium deposits in the Great Divide Basin-Crooks Gap Area, Fremont and Sweetwater counties, Wyoming: Contr. to Geol., Wyoming Univ., v. 8, no. 2, pt. 1, p. 105-120.

Bale, W. D., Davies, E. W., Morgans, D. B., and Monk, C. B., 1957, The study of some ion-pairs by spectrophotometry: Discuss. Faraday Soc., v. 24, p. 94-102.

Berner, R. A., 1971, Principles of Chemical Sedimentology: New York, McGraw-Hill Book Co., 240 p.

Betts, R. H., 1955, Heat of hydrolysis of uranium IV in perchloric acid solutions: Canadian Jour. Chemistry, v. 33, p. 1775-1779.

Brookins, D. G., 1976, The Grants Mineral Belt, New Mexico: Comments on the coffinite-uraninite relationship, probable clay mineral reactions, and pyrite formation: New Mexico Geol. Soc. Spec. Pub. No. 6, p. 158-166.

Cheney, E. S. and Jensen, M. L., 1966, Stable isotope geology of the Gas Hills, Wyoming, Uranium District: Econ. Geol., v. 61, p. 44-71.

Cheney, E. S. and Trammell, J. W., 1973, Isotopic evidence for inorganic precipitation of uranium roll ore bodies: Am. Assoc. Petroleum Geol., v. 57, no. 7, p. 1297-1304.

Cole, D. L., Eyring, E. M., Rampton, D. T., Silzars, A., and Jensen, R. P., 1967, Rapid reaction rates in a uranyl ion hydrolysis equilibrium: Jour. Phys. Chem., v. 71, p. 2771-2775.

Cordfunke, E. H. P., 1964, Heats of formation of some hexavalent uranium compounds: Jour. Phys. Chem., v. 68, p. 3353-3356.

Cordfunke, E. H. P., Ouweltjes, W., and Prins, G., 1975, Standard enthalpies of formation of uranium compounds I. β-UO_3 and γ-UO_3: Jour. Chem. Thermo., v. 7, p. 1137-1142.

Cordfunke, E. H. P., Ouweltjes, W., and Prins, G., 1976, Standard enthalpies of formation of uranium compounds II. UO_2Cl_2 and UCl_4: Jour. Chem. Thermo., v. 8, p. 241-250.

Dahl, A. R. and Hagmair, J. L., 1974, Genesis and characteristics of the southern Powder River Basin uranium deposits, Wyoming, USA, in Formation of Uranium Ore Deposits: Internat. Atomic Energy Agency, Vienna, p. 201-218.

Davies, E. W. and Monk, C. B., 1957, Spectrophotometric studies of electrolytic dissociation, Part 4. Some uranyl salts in water: Trans. Faraday Soc., v. 53, p. 442-449.

Davis, J. F., 1969, Uranium deposits in the Powder River Basin: Contr. to Geol., Wyoming Univ., v. 8, no. 2, pt. 1, p. 131-142.

Deltombe, E., de Zoubov, N., and Pourbaix, M., 1956, Electrochemical behavior of uranium equilibrium voltage-pH diagrams of the system U-H_2O at 25°C: Cebelcor Rapp. Tech., no. 31, 14 p.

Denson, N. M., Bachman, G. O., and Zeller, H. D., 1959, Uranium-bearing lignite in northwestern South Dakota and adjacent states: U. S. Geol. Survey Bull., 1055B, p. 11-57.

Drobnič, M. and Kolar, D., 1966, Calorimetric determination of enthalpy of hydration of UO_2: Jour. Inorg. Nucl. Chem., v. 28, p. 2833-2835.

Eugster, H. P., 1970, Chemistry and origin of the brines of Lake Magadi, Kenya: Mineralog. Soc. Am. Spec. Paper, no. 3, p. 213-235.

Eugster, H. P. and Surdam, R. C., 1973, Depositional environment of the Green River Formation of Wyoming: A pre-report: Geol. Soc. Am. Bull., v. 84, p. 1115-1120.

Files, F. G., 1970, Geology and alteration associated with Wyoming uranium deposits: Ph.D. dissertation, Univ. California, Berkeley, 113 p.

Fischer, R. P., 1970, Similarities, differences, and some genetic problems of Wyoming and Colorado plateau types of uranium deposits in sandstone: Econ. Geol., v. 65, p. 778-784.

Fitzgibbon, G. C., Pavone, D., and Holley, C. E., Jr., 1972, Enthalpy of formation of uranium tetrachloride: Jour. Chem. Thermo., v. 3, p. 151-162.

Flotow, H. E. and Lohr, H. R., 1960, The heat capacity and thermodynamic functions of uranium from 5 to 350 K: Jour. Phys. Chem., v. 64, p. 904-906.

Fuger, J. and Oetting, F. L., 1976, The chemical thermodynamics of actinide elements and compounds. Pt. 2, The actinide aqueous ions: Internat. Atomic Energy Agency, Vienna, 65 p.

Garrels, R. M. and Christ, C. L., 1965, Solutions, Minerals, and Equilibria: San Francisco, California, Freeman, Cooper and Co., 450 p.

Garrels, R. M. and MacKenzie, F. T., 1971, Evolution of Sedimentary Rocks: New York, W. W. Norton and Co., Inc., 397 p.

Gayer, K. H. and Leider, H., 1955, The solubility of uranium trioxide, $UO_3 \cdot H_2O$, in solutions of sodium hydroxide and perchloric acid at 25°C: Jour. Am. Chem. Soc., v. 77, p. 1448-1450.

Gayer, K. H. and Leider, H., 1957, The solubility of uranium (IV) hydroxide in solutions of sodium hydroxide and perchloric acid at 25°C: Canadian Jour. Chem., v. 35, p. 5-7.

Goldenberg, N. and Amis, E. S., 1959, Equivalent conductance of electrolytes in mixed solvents. VI. Uranyl chloride in the water-ethanol system: Z. Physik. Chem. (Frankfurt), v. 22, p. 63-80.

Grandstaff, D. E., 1976, A kinetic study of the dissolution of uraninite: Econ. Geol., v. 71, p. 1493-1506.

Granger, H. C. and Warren, C. G., 1969, Unstable sulfur compounds and the origin of roll-type uranium deposits: Econ. Geol., v. 64, p. 160-171.

Granger H. C. and Warren, C. G., 1974, Zoning in the altered tongue associated with roll-type uranium deposits, in Formation of Uranium Ore Deposits: Internat. Atomic Energy Agency, Vienna, p. 185-200.

Greenberg, E. and Westrum, E. F., Jr., 1956, Heat capacity and thermodynamic functions of uranyl chloride from 6 to 350°K: Jour. Am. Chem. Soc., v. 78, p. 4526-4528.

Gruner, J. W., 1956, Concentration of uranium in sediments by multiple migration accretion: Econ. Geol., v. 51, p. 495-520.

Harshman, E. N., 1962, Alteration as a guide to uranium ore, Shirley Basin, Wyoming, in Short Papers in Geology, Hydrology, and Topography: U. S. Geol. Survey Prof. Paper 450-D, p. D8-D10.

Harshman, E. N., 1968a, Uranium deposits of Wyoming and South Dakota, in Ridge, J. D., ed., Ore Deposits of the United States, 1933-1967: New York, Am. Inst. Mining Metall. Petroleum Eng., v. 1, p. 816-831.

Harshman, E. N., 1968b, Uranium deposits of the Shirley Basin, Wyoming, in Ridge, J. D., ed., Ore Deposits of the United States, 1933-1967: New York, Am. Inst. Mining Metall. Petroleum Eng., v. 1, p. 850-856.

Harshman, E. N., 1972, Geology and uranium deposits, Shirley Basin Area, Wyoming: U. S. Geol. Survey Prof. Paper 745, 82 p.

Harshman, E. N., 1974, Distribution of elements in some roll-type uranium deposits, in Formation of Uranium Ore Deposits: Internat. Atomic Energy Agency, Vienna, p. 169-183.

Hart, O. M., 1968, Uranium in the Black Hills, in Ridge, J. D., ed., Ore Deposits of the United States, 1933-1967: New York, Am. Inst. Mining Metall. Petroleum Eng., v. 1, p. 832-837.

Helgeson, H. C., 1968, Evaluation of irreversible reactions in geochemical processes involving minerals and aqueous solutions - I. Thermodynamic relations: Geochim. et Cosmochim. Acta, v. 32, p. 853-877.

Helgeson, H. C., 1969, Thermodynamics of hydrothermal systems at elevated temperatures and pressures: Am. Jour. Sci., v. 267, p. 729-804.

Helgeson, H. C., 1970, A chemical and thermodynamic model of ore deposition in hydrothermal systems: Mineralog. Soc. Am. Spec. Paper 3, p. 155-186.

Helgeson, H. C., Brown, T. H., Nigrini, A., and Jones, T. A., 1970, Calculation of mass transfer in geochemical processes involving aqueous solutions: Geochim. et Cosmochim. Acta, v. 34, p. 569-592.

Helgeson, H. C., Garrels, R. M., and MacKenzie, F. T., 1969, Evaluation of irreversible reactions in geochemical processes involving minerals and aqueous solutions - II. Applications: Geochim. et Cosmochim. Acta, v. 3, p. 455-481.

Hostetler, P. B. and Garrels, R. M., 1962, Transportation and precipitation of uranium at low temperatures with special reference to sandstone uranium deposits: Econ. Geol., v. 57, p. 137-167.

Huber, E. J., Jr. and Holley, C. E., Jr., 1969, Enthalpies of formation of triuranium oxtaoxide and uranium dioxide: Jour. Chem. Thermo., v. 1, p. 267-272.

Huntzicker, J. J. and Westrum, E. F., Jr., 1971, The magnetic transition, heat capacity, and thermodynamic properties of uranium dioxide from 5 to 350 K: Jour. Chem. Thermo., v. 3, p. 61-76.

Jensen, M. L., 1958, Sulfur isotopes and the origin of sandstone-type uranium deposits: Econ. Geol., v. 53, p. 598-616.

Jones, W. M., Gordon, J., and Long, E. A., 1952, The heat capacities of uranium, uranium trioxide, and uranium dioxide from 15°K to 300°K: Jour. Chem. Phys., v. 20, p. 695-699.

King, J. W. and Austin, S. R., 1966, Some characteristics of roll-type uranium deposits at Gas Hills, Wyoming: Mining Eng., v. 18, no. 5, p. 73-80.

Klygin, A. E. and Smirnova, I. D., 1959, The dissociation constant of the $UO_2(CO_3)_3^{-4}$ ion: Russian Jour. Inorg. Chem., v. 4, p. 16-18.

Knight, J. E., 1976, A thermochemical study of alunite and copper-arsenic sulfosalt deposits: Unpublished M.S. thesis, Univ. Arizona, Tucson, 142 p.

Kraus, K. A. and Nelson, F., 1950, Hydrolytic behavior of metal ions. I. The acid constants of uranium (IV) and plutonium (IV): Jour. Am. Chem. Soc., v. 72, p. 3901-3906.

Kraus, K. A. and Nelson, F., 1955, Hydrolytic behavior of metal ions. IV. The acid constant of uranium IV as a function of temperature: Jour. Am. Chem. Soc., v. 77, p. 3721-3722.

Kraus, K. A. and Nelson, F., 1959, Anion exchange studies of metal complexes, in Hamer, W. J., ed., The Structure of Electrolytic Solutions: New York, John Wiley & Sons, Inc., p. 340-364.

Langmuir, D. and Applin, K., 1977, Refinement of the thermodynamic properties of uranium minerals and dissolved species with applications to the chemistry of ground waters in sandstone-type uranium deposits, in Campbell, J. A., ed., Short Papers of the U. S. Geological Survey Uranium Thorium Symp.: U. S. Geol. Survey Circ. 753, p. 57-66.

Latimer, W. M., 1952, The oxidation states of elements and their potentials in aqueous solutions: New York, Prentice Hall, Inc., 2nd ed., 392 p.

Lietzke, M. H. and Stoughton, R. W., 1960, The solubility of silver sulfate in electrolyte solutions. Part 7. Solubility in uranyl sulfate solutions: Jour. Phys. Chem., v. 64, p. 816-820.

Love, J. D., 1952, Preliminary report on uranium deposits in the Pumpkin Buttes area, Powder River Basin, Wyoming: U. S. Geol. Survey Circ. 176, 37 p.

McClaine, L. A., Bullwinkel, E. P., and Huggins, J. C., 1955, The carbonate chemistry of uranium: theory and applications: Internat. Conf. on the Peaceful Uses of Atomic Energy, v. 8, p. 26-37.

Melin, R. E., 1964, Description and origin of uranium deposits in Shirley Basin, Wyoming: Econ. Geol., v. 59, p. 835-849.

Melin, R. E., 1969, Uranium deposits in Shirley Basin, Wyoming: Contr. to Geol., Wyoming Univ., v. 8, no. 2, pt. 1, p. 143-149.

Mrak, V. A., 1968, Uranium deposits in the Eocene sandstones of the Powder River Basin, Wyoming, in Ridge, J. D., ed., Ore Deposits of the United States, 1933-1967: New York, Am. Inst. Mining Metall. Petroleum Eng., v. 1, p. 338-848.

Naumov, G. B., Ryzhenko, B. N., and Khodakovsky, I. L., 1974, Handbook of thermodynamic data: Natl. Tech. Inf. Service, Pb-226, 722/7GA, U. S. Dept. Commerce, 328 p.

Nelson, F. and Kraus, K. A., 1951, Chemistry of aqueous uranium (V) solutions. III. The uranium (IV)-(V)-(VI) equilibrium in perchlorate and chloride solutions: Jour. Am. Chem. Soc., v. 73, p. 2157-2161.

Nikitin, A. A., Sergeyeva, Z. I., Khodakovsky, I. L., and Nuamov, G. B., 1972, Uranyl hydrolysis in a hydrothermal region: Geokhimiya, no. 3, p. 297-307.

O'Cinneide, S., Scanlan, J. P., and Hynes, M. J., 1972, Overall stability constant of the complex $UO_2(CO_3)_3^{-4}$: Chem. Indus. (London), v. 50, p. 340.

Oetting, F. L., Rand, M. H., and Ackerman, R. J., 1976, The chemical thermodynamics of actinide elements and compounds. Part I. The Actinide Elements: Internat. Atomic Energy Agency, Vienna, 111 p.

O'Hare, P. A. G., Shinn, W. A., Mrazek, F. C., and Martin, A. E., 1972, Thermodynamic investigation of trisodium uranium V oxide (Na_3UO_4). I. Preparation and enthalpy of formation: Jour. Chem. Thermo., v. 4, p. 401-409.

Paces, T., 1972, Chemical characteristics and equilibration in natural water-felsic-rock-CO_2 system: Geochim. et Cosmochim. Acta, v. 36, p. 217-240.

Renfro, A. R., 1969, Uranium deposits in the Lower Cretaceous of the Black Hills: Contr. to Geol., Wyoming Univ., v. 8, no. 2, pt. 1, p. 87-92.

Rosholt, J. N. and Bartel, A. J., 1969, Uranium, thorium, and lead systematics in Granite Mountains, Wyoming: Earth and Planet. Sci. Letts., v. 7, no. 2, p. 141-147.

Rosholt, J. N., Harshman, E. N., Shields, W. R., and Garner, E. L., 1964, Isotopic fractionation of uranium related to roll features in sandstone, Shirley Basin, Wyoming: Econ. Geol., v. 59, p. 570-585.

Rossini, F. D., Wagman, D. D., Evans, W. H., Levine, S., and Jaffe, I., 1952, Selected values of chemical thermodynamic properties: Natl. Bur. Standards Circ. 500, U. S. Dept. Commerce, 268 p.

Rush, R. M., Johnson, J. S., and Kraus, K. A., 1962, Hydrolysis of uranium (VI): Ultracentrifugation and acidity measurements in chloride solutions: Inorg. Chem., v. 1, p. 378-386.

Sato, M., 1960, Oxidation of sulfide ore bodies. I. Geochemical environments in terms of Eh and pH: Econ. Geol., v. 55, p. 928-961.

Seaborg, G. T. and Katz, J. J., 1954, The Actinide Elements. Part I: New York, McGraw-Hill, Inc., 870 p.

Sergeyeva, E. I., Nikitin, A. A., Khodakovsky, I. L., and Naumov, G. B., 1972, Experimental investigation in the system UO_3-CO_2-H_2O in 25-200°C temperature interval: Geochemistry Internat., v. 9, p. 900-910.

Shawe, D. R. and Granger, H. C., 1965, Uranium ore rolls--an analysis: Econ. Geol., v. 60, p. 240-250.

Siever, R., 1957, The silica budget in the sedimentary cycle: Am. Mineralogist, v. 42, p. 821-841.

Sjöberg, E. L., 1976, A fundamental equation for calcite dissolution kinetics: Geochim. et Cosmochim. Acta, v. 40, p. 441-447.

Sobkowski, J., 1961, Oxidation-reduction potential of UO_2^{+2}-U^{+4} system II: Jour. Inorg. Nucl. Chem., v. 23, p. 81-90.

Spirakis, C. S., 1977, A theory for the origin of the Rifle-Garfield vanadium-uranium deposit, in Campbell, J. A., ed., Short Papers of the U. S. Geological Survey Uranium Thorium Symp.: U. S. Geol. Survey Circ. 753, p. 8-10.

Stuckless, J. S., Bunker, C. M., Bush, C. A., Doering, W. P., and Scott, J. H., 1977, Geochemical and petrological studies of a uraniferous granite from the Granite Mountains, Wyoming: Jour. Research U. S. Geol. Survey, v. 5, no. 1, p. 61-81.

Sugawara, K., 1967, Migration of elements through phases of the hydrosphere and atmosphere, in Vinogradov, A. P., ed., Chemistry of the Earth's Crust, v. 2: Israel Prog. for Sci. Trans., p. 501-510.

Tsymbal, C., 1969, Solution chemistry of uranium VI: Comm. Energ. At. (FR), Rapport CEA-R-3476, 99 p.

Van Zeggeren, F. and Storey, S. H., 1970, The Computation of Chemical Equilibria: Great Britain, Cambridge Univ. Press, 176 p.

Vidavskii, L. M. and Ippolitova, E. A., 1972, Heats of formation of uranium sulfate tetra and octahydrate: Radiokhimiya, v. 14, p. 129-131 (Russian).

Wagman, D. C., Evans, W. H., Parker, V. B., Halow, I., Bailey, S. M., Schumm, R. H., and Churney, K. L., 1971, Selected values of chemical thermodynamic properties: Natl. Bur. Standards Tech. Note 270-5, 37 p.

Wallace, R. M., 1967, Determination of stability constants by donnan membrane equilibrium: the uranyl sulfate complexes: Jour. Phys. Chem., v. 71, p. 1271-1276.

Warren, C. G., 1971, A method for discriminating between biogenic and chemical origins of the ore-stage pyrite in a roll-type uranium deposit: Econ. Geol., v. 66, p. 919-928.

Warren, C. G., 1972, Sulfur isotopes as a clue to the genetic geochemistry of a roll-type uranium deposit: Econ. Geol., v. 67, p. 759-767.

Warren, C. G. and Granger, H. C., 1973, The concept of growth and maturity of ore-stage pyrite in roll-type uranium deposits: Jour. Research U. S. Geol. Survey, v. 1, no. 2, p. 151-155.

Westrum, E. F., Jr. and Grønvold, F. J., 1959, Low temperature heat capacity and thermodynamic functions of triuranium octoxide: Jour. Am. Chem. Soc., v. 81, p. 1777-1780.

White, D. E., Hem, J. D., and Waring, G. A., 1963, Chemical composition of subsurface waters, data of geochemistry, 6th ed., Chap. F: U. S. Geol. Survey Prof. Paper 440-F, 67 p.